Ocean Engineering 250 (2022) 111030

Contents lists available at ScienceDirect

Ocean Engineering

journal homepage: www.elsevier.com/locate/oceaneng

Cross-flow vortex-induced vibration of a flexible fluid-conveying riser undergoing external oscillatory flow

Jinlong Duan [a], Jifu Zhou [a,b,*], Xu Wang [a], Yunxiang You [c], Xinglan Bai [d]

[a] CAS Key Laboratory for Mechanics in Fluid Solid Coupling Systems, Institute of Mechanics, Beijing, 100190, China
[b] School of Engineering Sciences, University of Chinese Academy of Sciences, Beijing, 100049, China
[c] State Key Laboratory of Ocean Engineering, Shanghai Jiao Tong University, Shanghai, 200240, China
[d] School of Naval Architecture and Maritime, Zhejiang Ocean University, Zhoushan, 316022, China

ARTICLE INFO

Keywords:
Vortex-induced vibration
Internal flow
External oscillatory flow
Flexible risers

ABSTRACT

Cross-flow (CF) vortex-induced vibration (VIV) of a flexible riser considering both internal flow and external oscillatory flow is numerically investigated with consideration of combining the structural model with semi-empirical hydrodynamic force model by using Finite Element Method. The accuracy of the applied model is firstly examined by comparing the numerical results with the experimental data, which proves that the model can reproduce typical characteristics of CF VIV of a flexible riser undergoing external oscillatory flow. Then CF VIV of a flexible fluid-conveying riser subjected to external oscillatory flow is studied while the non-dimensional internal flow velocity and density ratio between internal and external flows are changed. The results show that regardless of the non-dimensional internal flow velocity and density ratio, typical VIV features of a flexible riser, such as intermittent VIV, amplitude modulation, hysteresis, mode and frequency transitions as well as standing and travelling wave responses, can be captured with variation of external oscillatory flow velocity. Moreover, VIV developing process, including building-up, lock-in and dying-out, can be detected for CF VIV. With the increase of the non-dimensional internal flow velocity and density ratio, high mode response can be effortlessly triggered for CF VIV, which is accompanied with occurrence of new vibrating frequencies. In addition, the vibrating frequency of CF VIV decreases while the non-dimensional internal flow velocity and density ratio are increased.

1. Introduction

Flexible risers play an important role in transporting oil or mineral ores from seabed to sea surface in ocean engineering industry. While conveying oil or ocean minerals, the flexible risers are inevitably influenced by complicated environmental conditions, such as external ocean current and internal wave, thereby leading to vortex-induced vibration (VIV). Since VIV can cause structural fatigue which endangers the safety of deep-sea resource exploitation facilities, the mechanism and characteristics of VIV have been extensively investigated, experimentally and numerically (Sarpkaya (2004); Williamson and Govardhan (2008); Bearman (2011)).

VIV dynamics of flexible risers subjected to uniform and shear currents has drawn scholars' attention for decades. Hence, plenty of experiments and numerical simulation have been conducted by many researchers in order to investigate VIV mechanism and characteristics of flexible risers undergoing uniform (Song et al. (2011); Huera-Huarte et al. (2014); Xu et al. (2018)) or shear currents (Violette et al. (2010); Gao et al. (2015)). And experiment works of rigid bodies mainly include the oscillations of an elastically mounted rigid cylinder and of a rigid cylinder forced to vibrate. Among these researches, experiment of an elastically mounted rigid cylinder oscillation is mainly conducted to explored VIV mechanism and dynamics (Jauvtis and Williamson (2004); Govardhan and Williamson (2006); Blevins and Coughran (2009)). While the forced vibration experiment mostly aims to investigate the hydrodynamic force on the rigid body in order to establish useful hydrodynamic coefficient database (Gopalkrishnan (1993); Aronsen (2007); Dahl (2008)). Since interaction between real risers and fluid in ocean engineering is more complicated, experiments on VIV of flexible risers under various types of external flows have also thrived recently (Chaplin and King (2018); Yin et al. (2019); Zhang et al. (2021)). In these researches, both VIV response and hydrodynamic forces are

* Corresponding author. CAS Key laboratory for Mechanics in Fluid Solid Coupling Systems, Institute of Mechanics, Beijing, 100190, China.
E-mail address: zhoujf@imech.ac.cn (J. Zhou).

https://doi.org/10.1016/j.oceaneng.2022.111030
Received 7 May 2021; Received in revised form 26 January 2022; Accepted 4 March 2022
Available online 16 March 2022

analyzed and discussed with different parameters of structure or flow. For example, experiment work has been carried out by Trim et al. (2005) and Srinil et al. (2013), in which VIV characteristics of top tension flexible risers such as the dominating mode and frequency are mainly focused. Meanwhile, VIV response of steel catenary risers has also been studied experimentally by Chaplin and King (2018) and Zhang et al. (2021). During their research, both VIV dynamics and hydrodynamics with different external flow velocity are analyzed. Apart from these experiment works, many numerical studies based on Computational Fluid Dynamics (CFD) and semi-empirical method have been performed so that VIV with different parameters can be comprehensively investigated (Evangelinos et al. (2000); Bao et al. (2019); Chen et al. (2020); Li et al. (2020); Sun et al. (2020)). Semi-empirical models such as time-domain empirical hydrodynamic model and wake oscillator model are developed and modified by Thorsen et al. (2014), Thorsen et al. (2015) and Qu and Metrikine (2020), to reproduce the hydrodynamic force exerting on the flexible riser. Then VIV response is analyzed and discussed with these methods, including the root mean square (RMS) of displacement, dominating mode and frequency. Through these studies, typical VIV features are observed and analyzed while both the in-line (IL) and cross-flow (CF) responses are coupled. It is found that the dominating mode and frequency as well as the root mean square (RMS) of displacement in IL and CF directions can be changed with different parameters, such as the external flow velocity, the aspect ratio and the material property of the risers. In particular, risers subjected to shear current perform more complicated vibrations. For instance, due to the spatial variation of velocity, multi-mode and multi-frequency VIV responses are observed by Bourguet et al. (2011), Zhu et al. (2019a) and Wang and Xiao (2016). Mode transition occurs while different excited mode responses compete with each other, which is detected in the works of Li et al. (2018), Gao et al. (2019) and Bao and Chen (2021). All these founding can provide us with a good understanding of VIV mechanism and characteristics under uniform and shear currents.

However, it should be noticed that the environmental conditions during deep-sea resource exploitation are more complicated due to the winds, currents and waves. The flexible risers can be affected by not only the uniform and shear currents but also the time-varying incoming flows. As there exist periodic heave or surge motions for the offshore platforms, oscillatory flows can be generated and exerted on the deep-sea resource exploitation risers due to the relative motions between the flexible risers and the sea current. Recently, VIV dynamics of risers undergoing oscillatory flows has been studied experimentally and numerically. Compared with VIV under steady flow, VIV dynamics of risers exposed to oscillatory flow is much more complicated. Since the oscillatory flow velocity is time-dependent, the vortices shedding from the riser are suddenly reversed in direction with the reversal of oscillatory flow velocity. As a consequence, the hydrodynamic force exerting on the riser is also changed periodically. Besides, multi-mode VIV response can be excited due to the variation of oscillatory flow velocity. VIV under oscillatory flow with several key parameters, such as the Keulegan-Carpenter number (KC), Reynolds number (Re), reduced flow velocity (U_r) and Strouhal number (St), has been investigated. And the shedding vortices are found closely related to KC number (Williamson (1985); Obasaju et al. (1988)). Regardless of KC number, it is observed by Sumer and Fredsoe (1988) that the CF oscillation pattern of cylinders is notably affected by the vortex-shedding frequency before lock-in occurs. Similarly, multi-frequency CF VIV response is also detected under oscillatory flow by Zhao (2013)., and the increase of U_r plays a determined role in the decrease of vibrating frequencies. Recently, depending on KC, three developing processes for VIV in oscillatory flow, including building-up, lock-in, and dying-out, as well as intermittent VIV are obtained by Fu et al. (2014), Thorsen et al. (2016), Wang et al. (2018) and Fu et al. (2018). Besides, mode transition occurs frequently due to the change of the oscillatory flow velocity, which is also observed by Yuan et al. (2018) and Xue et al. (2019). Obviously, these researches enrich the knowledge of VIV under external oscillatory flow.

Although VIV dynamics of risers have been widely researched, all these aforesaid investigations focus on VIV with only different types of external flows. Since the flexile risers are utilized to transport oil or mineral ores from seabed to sea surface, additional forces induced by the internal flowing mixtures can be exerted on these risers. And such forces have been proved to have a significant effect on the structural dynamics. For example, Wang et al. (2012), Kheiri et al. (2014) and Païdoussis (2014) have proved that when there exists internal flow inside, complicated dynamics, such as riser instability, quasi-periodic and chaotic vibrations, can be detected with high internal flow velocity. Therefore, based on the above statement, it can be concluded that the influence of both internal and external flows on VIV should not be ignored. While VIV mechanism and characteristics of the flexible risers are investigated, the combination of internal and external flows should be taken into consideration.

Recently, by considering the coupling of internal flow and external uniform currents, VIV dynamics has been explored with the variation of internal flow velocity. During their investigations, VIV response is found remarkably affected by the internal flow. The existence of the internal flow can decrease the natural frequency of the riser and increase the vibrating amplitudes, as demonstrated in the experiments of Guo and Lou (2008), Zhu et al. (2018) and Zhu et al. (2019b). Besides, as one of the dominant factors, the internal flow velocity can have a notable influence on some VIV response, such as lock-in and mode transition as well as standing and travelling wave response (Meng et al. (2017); Wang et al. (2018); Duan et al. (2018); Yang et al. (2018); Jiang et al. (2019)). Moreover, it has been proved by Thorsen et al. (2019), Li et al. (2020), Liang and Lou (2020) and Duan et al. (2021a, 2021b) that the internal fluid density can affect VIV dynamics, including the dominating mode and frequency. Nevertheless, in these studies, the internal flow and external steady current are mostly considered. In addition to uniform and shear currents, complicated external flow exists due to wave-induced motion in real marine environment. Compared with that under steady flow, VIV response of the flexible risers with the combination of internal flow and external oscillatory flow is much more complicated due to the time-varying external flow velocity. And no report has been found on this subject to date. Therefore, the objective of this work is to investigate nonlinear VIV dynamics of a flexible riser considering internal flow and external oscillatory flow.

In present work, a VIV prediction model considering the combination of internal flow and external oscillatory flow is firstly proposed and elaborated. Then the accuracy of the model is examined based on the comparison of numerical and experimental results. The novelty of our work is to investigate nonlinear VIV dynamics of the flexible risers undergoing both internal flow and external oscillatory flow numerically. The paper is structured as follows. The applied structural model and time-domain hydrodynamic model is introduced and described in Section 2. Validations are made by comparing the numerical results with the experimental data in Section 3 so that the prediction accuracy of the coupling model is evaluated for VIV under oscillatory current. Then VIV response is explored numerically while the flexible fluid-conveying riser is subjected to oscillatory current in Section 4. Correspondingly, the change of VIV features with different non-dimensional internal flow velocity and density is examined. Finally, major conclusions are drawn in Section 5. It is worth mentioning that the main contributions of this paper are not developing an original model but investigating nonlinear CF VIV dynamics while the fluid-conveying riser undergoes complicated oscillatory flow outside, based on the existing VIV semi-empirical model. The aim here is to reveal typical CF VIV features and mechanism of a flexible fluid-conveying riser undergoing oscillatory flow during deep-sea resource exploitation.

2. Numerical model

2.1. Model of a flexible fluid-conveying riser undergoing external oscillatory flow

The flexible riser with both ends simply supported by hinges is considered as a flexural elastic structure transporting fluid inside. As shown in Fig. 1, x- and y-axis are assumed to be parallel and perpendicular to the incoming flow direction respectively and z-axis is along the riser's axial direction in the Cartesian coordinate system. The governing differential equation for VIV of the fluid-conveying riser in the CF direction can be expressed as Eq. (1) (Païdoussis (2014)):

$$\left(m_r + m_f + \frac{\pi}{4} C_a \rho_e D_e^2\right)\frac{\partial^2 y}{\partial t^2} + c_s\frac{\partial y}{\partial t} + 2m_f U_i \frac{\partial^2 y}{\partial z \partial t} + \left(m_f U_i^2 - T\right)\frac{\partial^2 y}{\partial z^2} + EI\frac{\partial^4 y}{\partial z^4} = F_{CF}(A^*, f^*, t) \tag{1}$$

where m_r and m_f are the riser mass and the internal flow mass per unit length of the riser. C_a is the added mass coefficient, equal to 1.0 here (Vandiver and Li (2018)). ρ_e denotes the density of the external flow. c_s represents the structural damping coefficient. A^* is the non-dimensional CF vibrating amplitude to riser's external diameter D_e. f^* is the non-dimensional frequency, which can be obtained by $f^* = fD_e/\ U_e$ based on the CF vibrating frequency f and external flow velocity U_e. E and I represent the elastic modulus and moment of inertia respectively. T is the effective axial tension. F_{CF} is the VIV exciting force in CF direction.

It should be noticed from the governing equation that there does not exist direct coupling effect between external and internal flows for VIV here. This can be explained by that the internal flow just has an impact on the structure motion property rather than interacts with the external flow directly. As a result, no direct coupling effect between external and internal flows is considered in our model. According to Païdoussis (2014), the third and fourth terms of the governing equation represents the effect of internal flow exerting on CF VIV of the flexible fluid-conveying riser. The third term indicates the impact of Coriolis force caused by the internal fluid flowing in the vibrating riser, which can exert an excitation or damping effect on VIV under different conditions. While the fourth term in the governing equation denotes the centrifugal force effect induced by the internal flow in the bended riser, which can change the stiffness of the flexible fluid-conveying riser. Therefore, the internal flow exerts an impact on VIV response through the change of riser stiffness as well as excitation or damping effect.

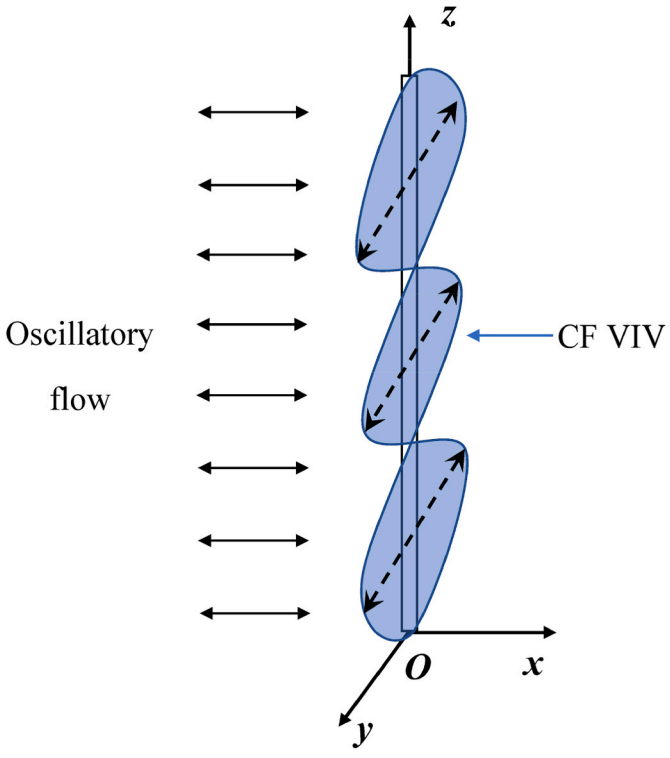

Fig. 1. Schematic of the flexible fluid-conveying riser subjected to external oscillatory flow.

Meanwhile, the effect of external oscillatory flow can be reflected in the right side of the governing equation, e.g., the external hydrodynamic force term. And the existence of all the terms in the governing equation indicates that the effect of internal and external flows on CF VIV has been taken into account in the proposed model.

2.2. Identification of exciting and damping periods

The hydrodynamic force exerting on the flexible riser in CF direction can be either exciting force or damping force according to the identification of exciting and damping periods under oscillatory current. Since the external flow velocity is time-varying for oscillatory current, the exciting and damping periods are required to be determined with the time progressing so that either the exciting or damping force can be exerted on the flexible riser during the specific period. The reduced velocity has been proved as an effective criterion to distinguish the exciting and damping periods of the flexible riser under uniform, shear and oscillatory currents (Vandiver and Li (2018)). Therefore, the exciting and damping periods under oscillatory current are identified based on the reduced velocity here. And the identification criterion is expressed as:

$$V_{r,i}^{min} \le V_{r,i}(t) \le V_{r,i}^{max} \text{ exciting period}$$

$$V_{r,i}(t) < V_{r,i}^{min} \text{ or } V_{r,i}(t) > V_{r,i}^{max} \text{ damping period}$$

where $V_{r,i}$ is the reduced velocity of mode i, which can be determined by the following equation:

$$V_{r,i}(t) = \frac{f_i |U_e(t)|}{D_e} \tag{2}$$

where f_i is the natural frequency of mode i. $V_{r,i}^{min}$ and $V_{r,i}^{max}$ are respectively the lower and upper limits of the reduced velocity range between which mode i can be excited. The sketch of the exciting and damping periods under oscillatory current is illustrated in Fig. 2, which can provide a better understanding.

Based on the recently published experimental research by Zheng (2014), semi-empirical model, in which non-dimensional frequency range of [0.125, 0.25] is regarded as the lock-in region for CF VIV response, can predict VIV dynamics better. Hence, the non-dimensional frequency range of [0.125, 0.25] is adopted as the lock-in region during our simulation. The non-dimensional frequency can be calculated by $f^*(t) = \frac{f_i D_e}{|U_e(t)|}$. Correspondingly, the reduced velocity range of [4, 8] is determined as lock-in region. Due to the change of Reynolds number, the non-dimensional frequency is required to modify based on the real

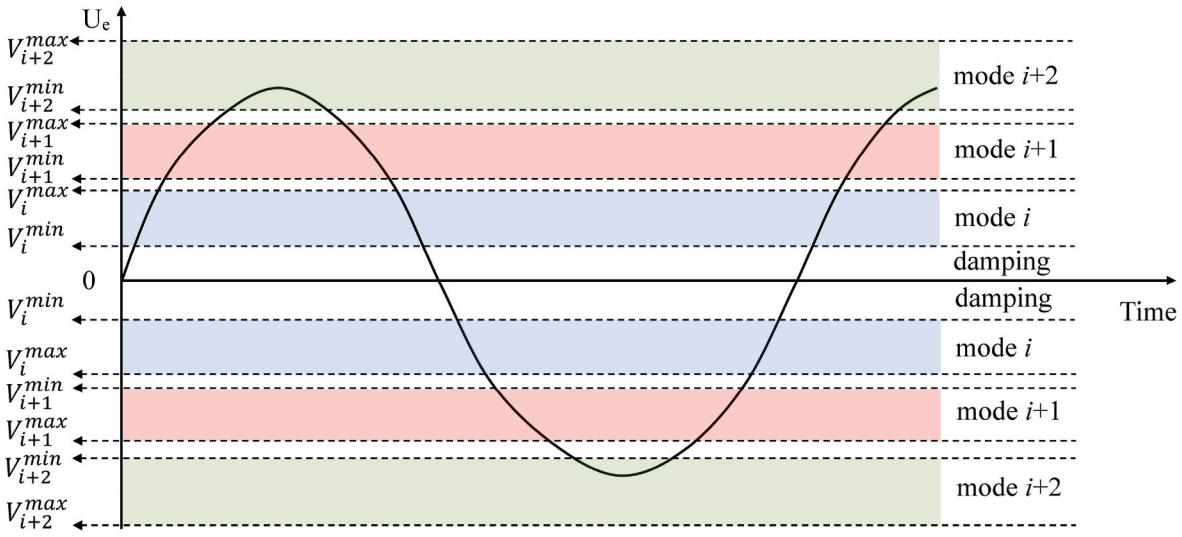

Fig. 2. Schematic of excited mode response with the variation of oscillatory flow velocity.

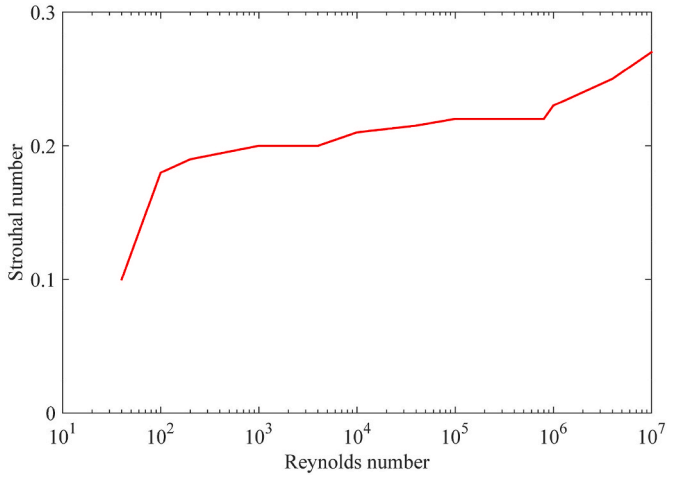

Fig. 3. Strouhal number as function of Reynolds number (Passano et al. (2016)).

Reynolds number so that the appropriate Strouhal number can be obtained, as shown in Fig. 3 (Passano et al. (2016)) Then the modified non-dimensional frequency is calculated:

$$f_G^*(t) = \frac{St \cdot f^*(t)}{St^*} \tag{3}$$

where $St = 0.19$ and St^* is the Strouhal number obtained based on the real Reynolds number. It should be noted that $St = 0.19$ is not always suitable due to the change of real Reynolds number. Hence, the Strouhal number value is modified according to Reynolds number during the calculation (Fig. 3). Then appropriate non-dimensional frequency can be obtained. After the non-dimensional frequency is modified, the exciting and damping periods of the flexible riser under oscillatory current can be identified.

2.3. Hydrodynamic force in exciting and damping periods

While VIV occurs in oscillatory flow, the vortex-shedding regimes are found distinct from those under steady flows. Studies have proved that during each half period of the oscillatory motion, vortex shedding occurs closely dependent on the KC number. As the cylinder undergoes oscillatory flow, vortices newly shed from it might not be evolved entirely when the flow tend to reverse, causing that vortices in the wake field are washed reversely over the cylinder. Then due to its self-induced velocity field, these latest vortex pairs convect away from the cylinder in the direction not accordance to the cylinder motion. Moreover, the number of vortex pairs convecting away from the cylinder is increased with the increase of KC number (Sumer and Fredsoe (2006)).

Unlike steady flow, since there exist vortex pairs moving away from the cylinder in various directions when flow reversal occurs, frequency of vortex shedding is not quite straightforward in oscillatory flows, especially for lower KC numbers. For KC numbers less than 30, the vortex shedding period accounts for an appreciable portion in the flow oscillation period and interaction between the vortex shedding and flow oscillation exists strongly. Nevertheless, with the increase of KC numbers, the portion of the vortex shedding period in the flow oscillation period decreases gradually. As a result, the vortex shedding period becomes a small fraction of the flow oscillation period when the KC number is above 30. Correspondingly, steady flow vortex shedding data can be applied using the instantaneous of flow velocity for KC numbers above 30 (Blevins (1990)). In addition, it has been proved that VIV characteristics, such as a resonant response, a lock-in band and a self-limiting maximum amplitude can be produced when vortex shedding occurs in both oscillatory and steady flows. Therefore, hydrodynamic coefficient data based on steady flow can be reasonably utilized for oscillatory flow cases, at least at higher KC numbers (Blevins (1990); Sumer and Fredsoe (2006)). Since the KC numbers in our investigation are approximately 31, 178 and 524, the hydrodynamic coefficient database that has been obtained under steady flows is used to calculate the hydrodynamic force on the flexible riser exposed to external oscillatory flow.

Similar to VIV under steady flow, after the exciting period is determined, the hydrodynamic force is required to exert on the flexible riser during this certain period. The hydrodynamic force of mode i acting on the flexible riser in exciting period can be expressed as (Blevins (1990)):

$$F_{CF,i} = \frac{1}{2} C_{L,CF,i}(A^*, f_i^*, t) \rho_e D_e U_e(t)^2 \cos(\omega_{CF,i} \cdot t) \tag{4}$$

where $C_{L,CF,i}(A^*, f_i^*, t)$ is the hydrodynamic force coefficient in the exciting period of the i^{th}-order excitation frequencies in CF direction, which is related to the non-dimensional vibration amplitude and frequency of the excited mode i as well as current time. ρ_e is the density of the external oscillatory flow. $\omega_{CF,i}$ represents the natural frequency for mode i response. In order to keep the hydrodynamic force and the structural velocity in phase while mode i response is triggered, the hy-

drodynamic force of mode i exerting on the flexible riser can be rewritten as:

$$F_{CF,i}=\frac{1}{2}C_{L,CF,i}\left(A^*,f_i^*,t\right)\rho_e D_e U_e(t)^2\frac{\dot{y}(t)}{\dot{y}_m} \tag{5}$$

where $\dot{y}(t)$ denotes the CF velocity of mode i response at t. And $\dot{y}_m$ represents the CF VIV velocity amplitude of mode i response in latest period.

As far as we are concerned, there exists strong complexity and nonlinearity of the ambient flow while VIV of a flexible riser occurs. Not only three-dimensional hydrodynamic coupling effect due to the nonlinear flow is exerted along the flexible riser, but also the flow nonlinearity is enhanced as VIV dynamics affects the flow in turn. Therefore, it is very difficult to establish a database of hydrodynamic coefficient which can be suitable for all kinds of risers under various environmental conditions. As a result, there is no available hydrodynamic coefficient database at present for VIV of flexible risers undergoing complicated external flow. Hence, the hydrodynamic database from VIVANA is widely applied because of the absence of available hydrodynamic coefficients for flexible risers while VIV of flexible risers subjected to different types of external flow, such as uniform, shear and oscillatory flows, is investigated. Similarly, the hydrodynamic force coefficient $C_{L,CF,i}(A^*,f_i^*,t)$ in exciting period here can be obtained based on the database in VIVANA (Passano et al. (2016)). Although this database is originated from forced vibration experimental data by Gopalkrishnan (1993), the application of the hydrodynamic database in VIVANA has been proved feasibility and acceptable for VIV under oscillatory current, for example in the works by Thorsen et al. (2016), Yuan et al. (2018), Xue et al. (2019), Lu et al. (2019) and Yuan et al. (2020a, 2020b). Therefore, $C_{L,CF,i}(A^*,f_i^*,t)$ corresponding to certain current, non-dimensional frequency and time can be selected from the aforesaid database, as shown in Fig. 4. Then the instantaneous $C_{L,CF,i}(A^*, f_i^*,t)$ in exciting period can be calculated according to the curve fitted in Fig. 5.

The hydrodynamic damping model proposed by Thorsen et al. (2016) for flexible risers undergoing VIV with various kinds of flow current is adopted during our simulation. It is related to the CF velocity of the flexible riser, expressed as

$$F_{damp}=-\frac{1}{2}\rho_e D_e C_{damp}|\dot{y}|\dot{y} \tag{6}$$

where C_{damp} denotes the damping coefficient during the damping period. According to Thorsen et al. (2016), the damping coefficient is closely related to the CF amplitude, which can be obtained by $C_{damp}=a_0+a_1\frac{y}{D_e}$. Based on the comparison of the numerical and experiment results, the model with $a_0=0.31$ and $a_1=0.89$ can yield a good approximation

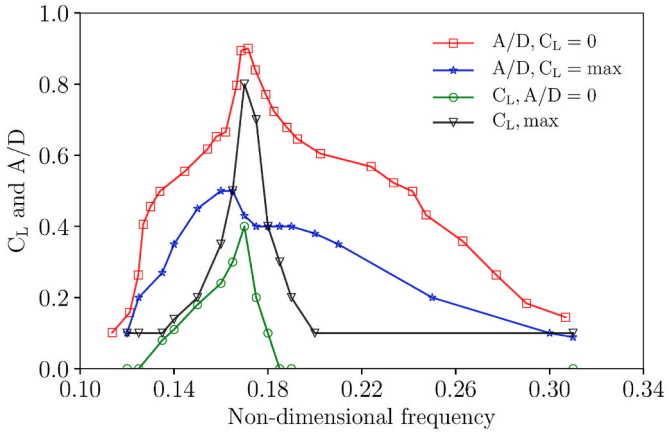

Fig. 4. The excitation coefficients for CF VIV (Passano et al. (2016)).

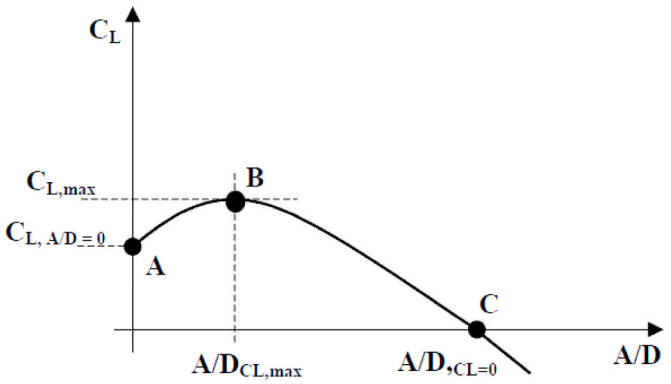

Fig. 5. Function of the excitation coefficient vs nondimensional amplitude.

of the hydrodynamic damping force (Thorsen et al., 2016). Therefore, $C_{damp}=0.31+0.89\frac{y}{D_e}$ is applied here.

2.4. Solution and calculation procedures

By using the finite element method, the governing equation of the flexible riser considering the internal flow and external oscillatory current is discretized. After discretization, the governing equation for VIV of the flexible riser can be expressed as:

$$\mathbf{M}\ddot{y}(t)+\mathbf{C}\dot{y}(t)+\mathbf{K}y(t)=\mathbf{F}(t) \tag{7}$$

where **M** is the total mass matrix, including the added mass and internal flow mass. **C** and **K** are the total structural damping matrix and the total stiffness matrix with consideration of the internal flow effect. The Rayleigh damping model is utilized to calculating the damping matrix **C**. And the first and second dominant mode frequencies of the flexible riser is applied to calculate the parameters of Rayleigh damping model. Then the discretized equation is solved by using Newmark-β method.

The calculating procedure is illustrated in Fig. 6 so that the process of the time domain analysis can be understood clearly. As is demonstrated, the hydrodynamic coefficients depend closely on the instantaneous vibrating amplitude and frequency of the flexible riser and are updated every vibrating circle of the flexible riser. Then based on the updated hydrodynamic coefficients, the instantaneous hydrodynamic forces are calculated and applied to simulate VIV response of the flexible fluid-conveying riser subjected to external oscillatory flow. Before the simulation, element number and timestep convergences have been carried out. Numerical results with various element numbers and timesteps have been examined. With consideration of both accuracy and computing efficiency, the element number of the flexible fluid-conveying riser and calculating timestep are set 100 and 0.01s respectively in our simulation (Duan et al. (2021a)).

3. Model validation by comparing with experiment

In order to examine the accuracy of the model, validation is carried out based on the comparison of the numerical and experimental results. Correspondingly, the experiment data of VIV dynamics of a flexible riser undergoing oscillatory flow obtained by Fu et al. (2014) are chosen here. Without considering the internal flow, numerical simulation of VIV of the flexible riser subjected to external oscillatory flow is conducted by using the proposed model. The main parameters of the flexible riser are listed in Table 1. Detailed information of the experiment can be found in Fu et al. (2014).

The experiment was conducted by towing the flexible riser with certain oscillation motion horizontally. Therefore, the oscillatory flow velocity can be expressed as (Fu et al. (2014))

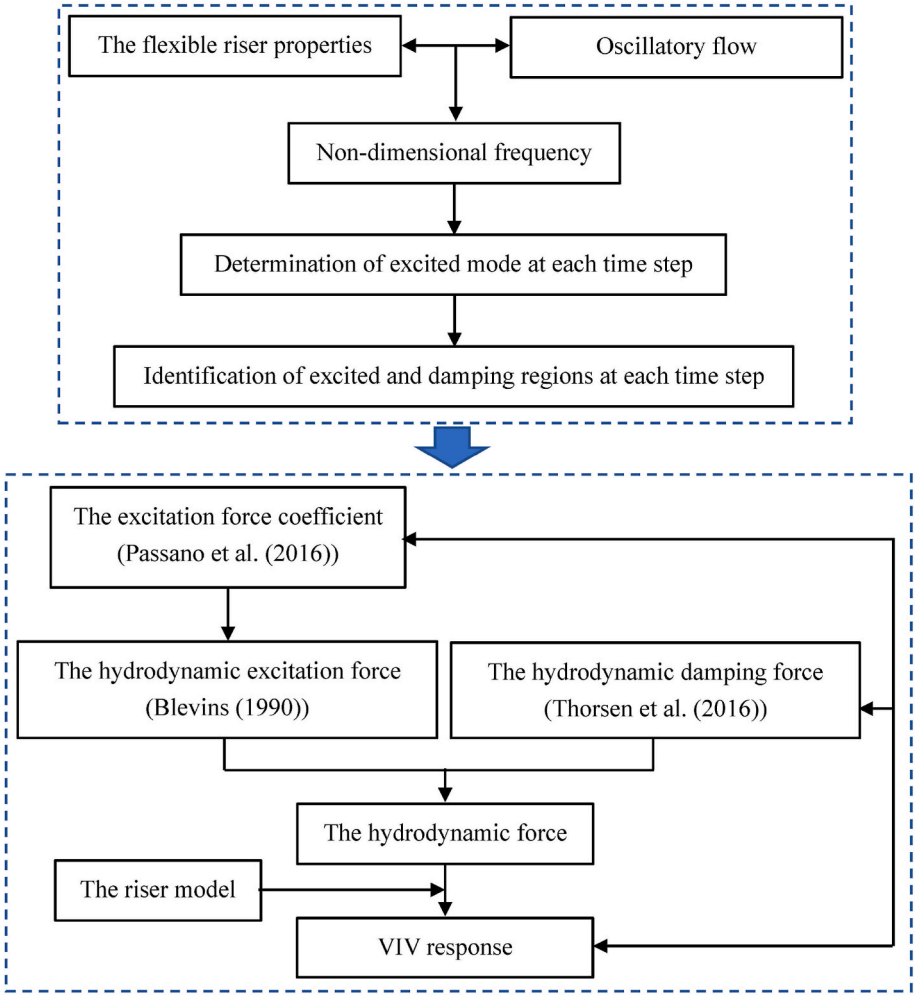

Fig. 6. Calculation procedure of the present model.

Table 1
Parameters of the flexible riser model (Fu et al. (2014)).

Parameter	Value
Length L (m)	4.0
Bending stiffness EI (N · m^2)	10.5
Outer diameter D_e (m)	0.024
Pretension T (N)	500
Mass per unit m_r (kg)	0.69
Damping ratio c	0.015

$$U(t) = A_m \frac{2\pi}{T} \cos\left(\frac{2\pi}{T} t\right) \tag{8}$$

where A_m denotes the maximum oscillation motion amplitude, T represents the period of the oscillation motion. As for the oscillatory flow, Keulegan-Carpenter (KC) number can be defined as follows:

Table 2
Cases for validation.

Case	A_m (m)	T (s)	KC number
1	0.68	16.5	178
2	0.68	10.2	178
3	0.68	8.45	178
4	0.12	2.5	31
5	0.12	1.8	31
6	0.12	1.45	31

$$KC = \frac{U_m T}{D_e} = \frac{2\pi A_m}{D_e} \tag{9}$$

where U_m is the maximum velocity of the oscillatory flowing and D_e denotes the external diameter of the flexible riser.

During the experiment, tests considering a series of KC numbers and reduced velocities were carried out. In this section, six cases with KC number equal to178 and 31 are chosen for the validation, as shown in Table 2. Correspondingly, the vibration time history and frequency of the flexible riser are mainly focused and analyzed based on the continuous wavelet transform technique.

It can be seen from Figs. 7–12 that for different KC numbers, the proposed model can capture the main VIV characteristics of the flexible riser undergoing external oscillatory flow, such as the intermittent VIV, amplitude modulation and VIV developing process. With high KC number, VIV developing process can be evidently distinguished, including building-up, lock-in and dying-out, which can also be obtained in the experiment of Fu et al. (2014) as well as the simulation works of Yuan et al. (2018), Thorsen et al. (2016) and Lu et al. (2019). Note that under steady flow, lock-in refers to the VIV response occurring when the vortex shedding frequency is locked onto the specific structural frequency. But in terms of external oscillatory flow, intermittent VIV dominates the response which is mainly characterized by three processes: building-up, lock-in and dying-out. Although the oscillatory flow velocity is time-varying, the oscillatory flow velocity can increase or decrease mildly in a certain period. As a consequence, the vortex shedding frequency is locked onto one specific natural frequency of the

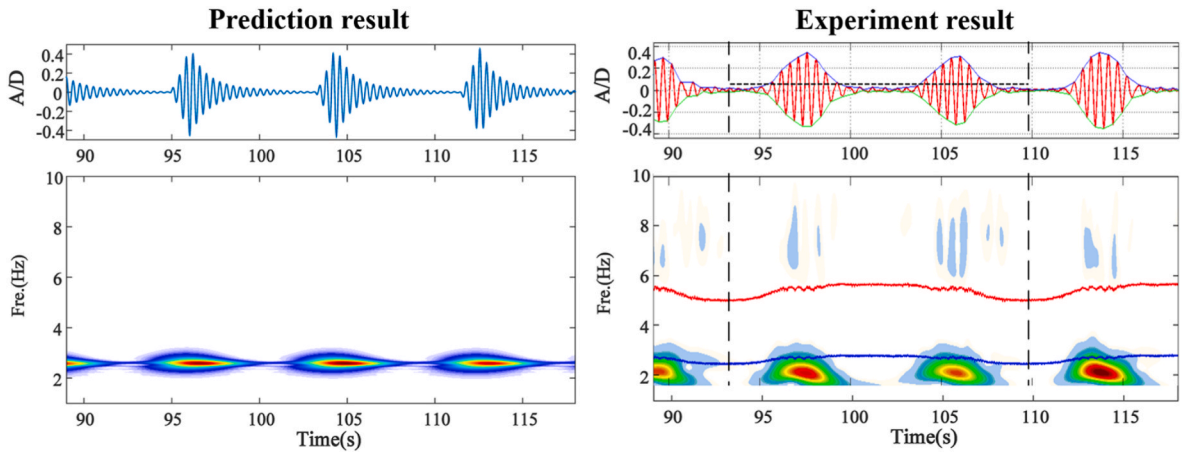

Fig. 7. Comparison between prediction and experiment results for Case 1 ($A_m = 0.68$ m and $T = 16.5$ s). The top row presents the non-dimensional displacement of CF VIV and the bottom row shows the frequency distribution over time at $z = 2$ m.

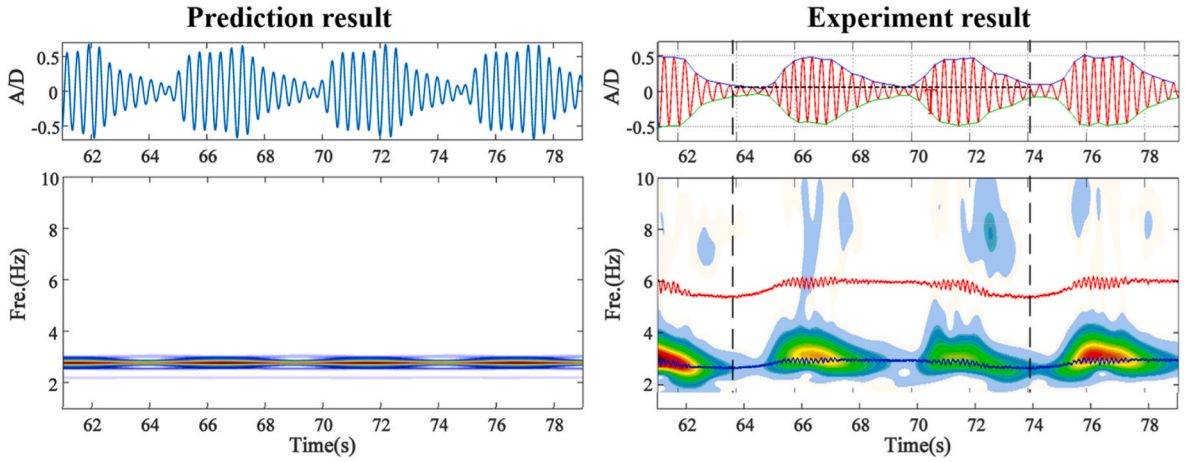

Fig. 8. Comparison between prediction and experiment results for Case 2 ($A_m = 0.68$ m and $T = 10.2$ s). The top row presents the non-dimensional displacement of CF VIV and the bottom row shows the frequency distribution over time at $z = 2$ m.

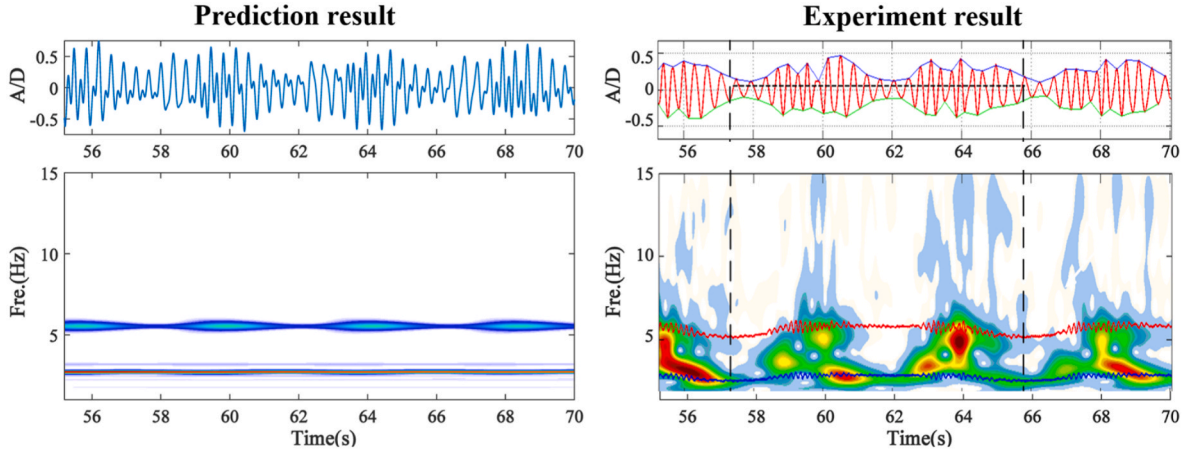

Fig. 9. Comparison between prediction and experiment results for Case 3 ($A_m = 0.68$ m and $T = 8.45$ s). The top row presents the non-dimensional displacement of CF VIV and the bottom row shows the frequency distribution over time at $z = 1$ m.

riser, resulting in lock-in. When lock-in phenomenon under oscillatory flow occurs, typical VIV characteristics can be captured, which is similar to those under steady flow. It should be noticed that the occurrence of lock-in under oscillatory flow is time-dependent due to the change of flow velocity. While the oscillatory flow velocity changes dramatically, building-up and dying-out processes dominate VIV response. Meanwhile, the dominating frequency and maximum amplitudes of VIV show a good agreement with the experimental data, which proves the high

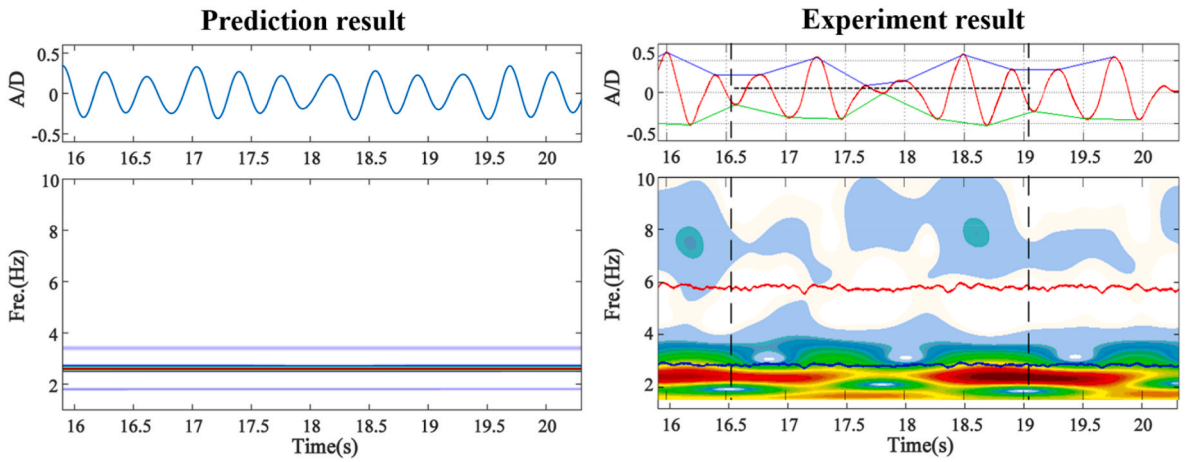

Fig. 10. Comparison between prediction and experiment results for Case 4 ($A_m = 0.12$ m and $T = 2.5$ s). The top row presents the non-dimensional displacement of CF VIV and the bottom row shows the frequency distribution over time at $z = 2$ m.

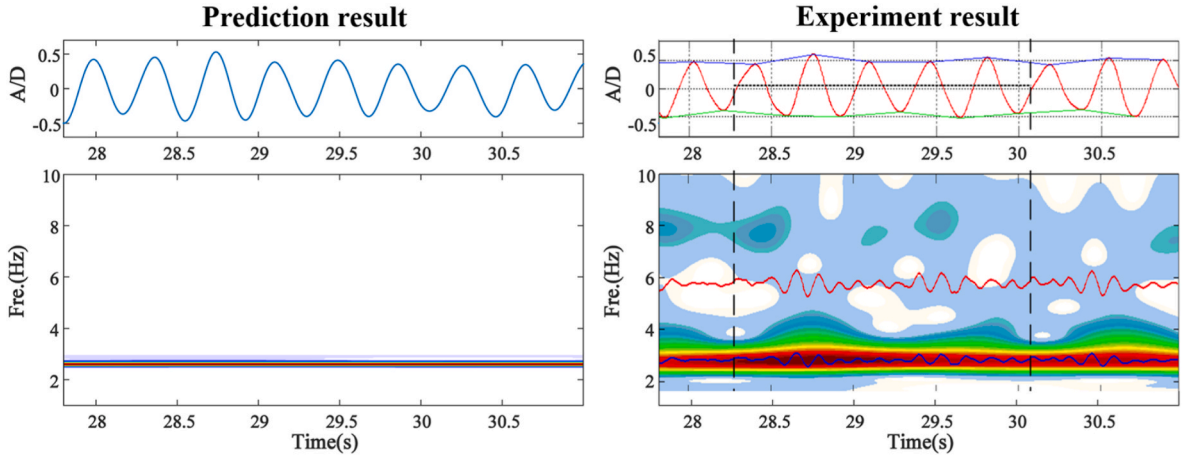

Fig. 11. Comparison between prediction and experiment results for Case 5 ($A_m = 0.12$ m and $T = 1.8$ s). The top row presents the non-dimensional displacement of CF VIV and the bottom row shows the frequency distribution over time at $z = 2$ m.

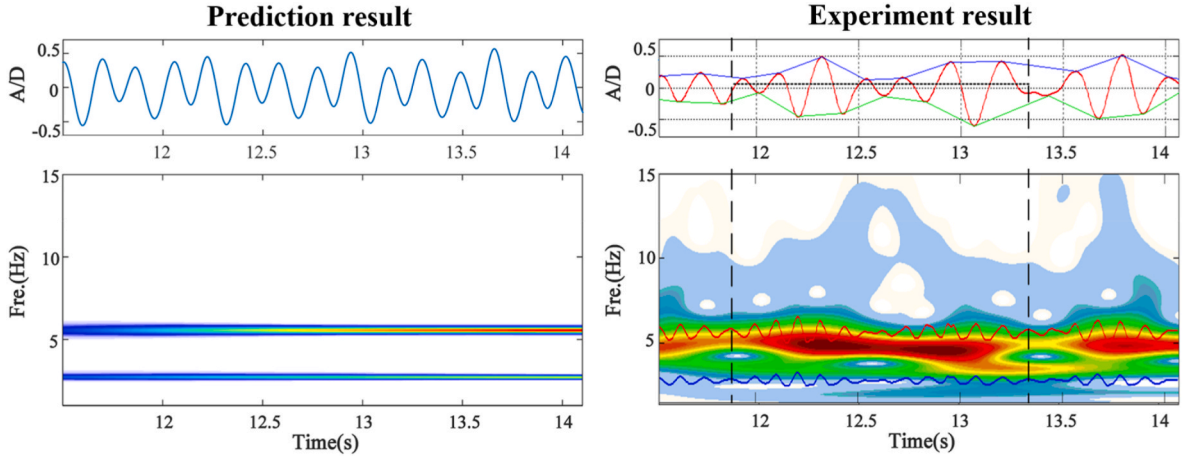

Fig. 12. Comparison between prediction and experiment results for Case 6 ($A_m = 0.12$ m and $T = 1.45$ s). The top row presents the non-dimensional displacement of CF VIV and the bottom row shows the frequency distribution over time at $z = 1$ m.

accuracy of the proposed model. Besides, multi-frequency vibration is also detected during the simulation. Overall, it can be concluded that the proposed model can capture main CF VIV characteristics of a flexible riser subjected to oscillatory flow with different KC numbers.

4. CF VIV dynamics of the flexible fluid-conveying riser undergoing external oscillatory flow

It has been proved in previous section that CF VIV dynamics of the flexible riser exposed to external oscillatory flow can be predicted by the proposed model when the internal flow is not taken into account. Therefore, it is reasonable to assume that the results remain true when the flexible riser transports flow inside. Since the inner diameter of the flexible riser is not given by Fu et al. (2014), it is assumed to be equal to 0.02m while the internal flow is considered. And the external flow density is set to equal to 1000kg/m^3. When CF VIV of the flexible fluid-conveying riser is focused with the increase of internal flow velocity, the density of internal flow is assumed to be 1000kg/m^3. And the non-dimensional internal flow velocity is set to equal to 5 while CF VIV is investigated with the increase of density ratio of internal and external flows. Note that only the first and second mode responses of CF VIV response are excited in the experiment of Fu et al. (2014). In order to investigate the effect of internal flow on CF VIV dynamics of the flexible riser undergoing external oscillatory flow, the maximum oscillatory flow velocity is increased here so that CF VIV characteristics with different internal flow parameters can be evidently revealed. Hence, the main parameters of the oscillatory flow are changed as follows: $A_m = 2$m and $T = 10$s. Since this study concentrates on the influence of the internal flow on CF VIV, some parameters of the external oscillatory flow, such as KC number and period, are constant during our simulation. As shown in Fig. 13, the first four mode responses can be triggered during one period of the external oscillatory flow while the internal flow is not considered. Correspondingly, the excited mode, frequency, VIV developing process as well as standing and travelling wave responses are mainly focused and analyzed by changing the non-dimensional velocity of the internal flow and density ratio of the internal and external flows.

According to Païdoussis (2014), the non-dimensional internal flow velocity can be defined as $u = \sqrt{\frac{m_f}{EI}} \cdot LU_i$. And the density ratio of the internal and external flows can be expressed as $\beta = \frac{\rho_i}{\rho_e}$.

4.1. The excited modes for CF VIV considering internal flow and external oscillatory flow

Modal decomposition is applied for the CF VIV response of the flexible fluid-conveying riser under external oscillatory flow so that the dominating mode with the time variation can be obtained under different non-dimensional internal flow velocity. A sum of mode shapes with different modal weights is used to describe the CF displacement of the riser, which is expressed as

$$y(z,t) = \sum_{n=1}^{\infty} w_n(t)\varphi_n(z) = \sum_{n=1}^{\infty} w_n(t)\sin\left(\frac{n\pi z}{L}\right) \tag{10}$$

where $w_n(t)$ denotes the modal weight of the CF displacement, z denotes the axial position along the riser and $\varphi_n(z)$ represents the n th modal shape. By using this method, the modal weight of the CF displacement for various mode responses can be obtained.

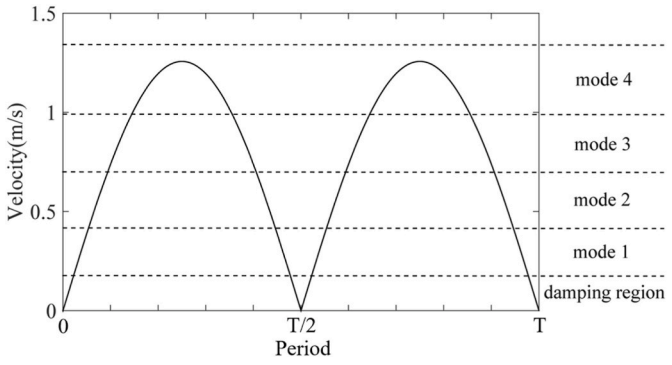

Fig. 13. The expected mode response excited with the variation of oscillatory flow velocity.

4.1.1. The excited modes with different non-dimensional internal flow velocities

As shown in Fig. 14, the modal weights corresponding to the first six mode VIV responses within one period of oscillatory flow are illustrated while the non-dimensional internal flow velocity u is increased. It can be seen that regardless of the non-dimensional internal flow velocity, various mode responses of VIV in CF direction are triggered during one period of oscillatory flow. Take $u = 0$ as an example, in which the flexible riser is filled with still internal flow. When the external oscillatory flow velocity is at low values, the CF VIV is mainly dominated by the 1st mode response. With the increase of the oscillatory flow velocity, mode transition occurs. The dominated VIV response changes from mode 1 to mode 2, then to mode 3 before the external oscillatory flow velocity reaches its maximum. While the oscillatory flow velocity is firstly approaching to its maximum and then decreases, the 4th mode response takes over the CF VIV dynamics till the 3rd mode response is excited again. As the external oscillatory flow velocity keeps decreasing, CF VIV is dominated by 2nd mode response again, then by 1st mode response.

Note that each mode response is almost characterized by three developing processes: building-up, lock-in and dying-out. Since the duration time of each dominated mode response is various, lock-in process of the corresponding mode response might not be notably detected for some dominated mode responses. This phenomenon can be obviously observed for the 1st, 2nd and 3rd mode CF VIV responses with $u = 0$. By contrast, building-up and dying-out can be evidently observed with time variation for all the dominated mode responses. The excitation of various mode VIV responses in CF direction for the flexible riser undergoing external oscillatory flow can be attributed to that different mode responses are triggered with the change of the oscillatory current velocity. As a result, CF VIV dynamics is dominated by different mode responses while the external oscillatory flow velocity is increased or decreased.

Meanwhile, hysteresis can be predicted for CF VIV of the fluid-conveying riser subjected to external oscillatory flow. Hysteresis is defined by Fu et al. (2014) as that in one period of the external oscillatory flow, the VIV amplitude values corresponding to the same current velocity in both the acceleration and deceleration processes of the external oscillatory flow current are not equal, with the former value less than the latter one. In other word, the VIV amplitude builds up faster than it dies out. Such phenomenon is very notable for the 4th dominated mode response with $u = 0$ and 5, as shown in Fig. 14. The existence of hysteresis can be explained by that when mode transition occurs, the dominated mode response corresponding to the current oscillatory flow velocity is excited, which is accompanied with the former one decaying. As the decaying process needs time, there appears the superposition of multi-mode responses for some intervals of time, especially for the moment with the occurrence of mode transition, which causes the enlargement of the vibrating amplitude in the deceleration process (Fig. 14). Consequently, hysteresis phenomenon arises.

What should be emphasized is that for CF VIV dynamics of the flexible riser with different non-dimensional internal flow velocity u, typical VIV characteristics, such as mode transition and VIV developing process, show a similar changing trend with the variation of external oscillatory flow velocity. However, the variation of the non-dimensional internal flow velocity can have an obvious effect on mode transition of

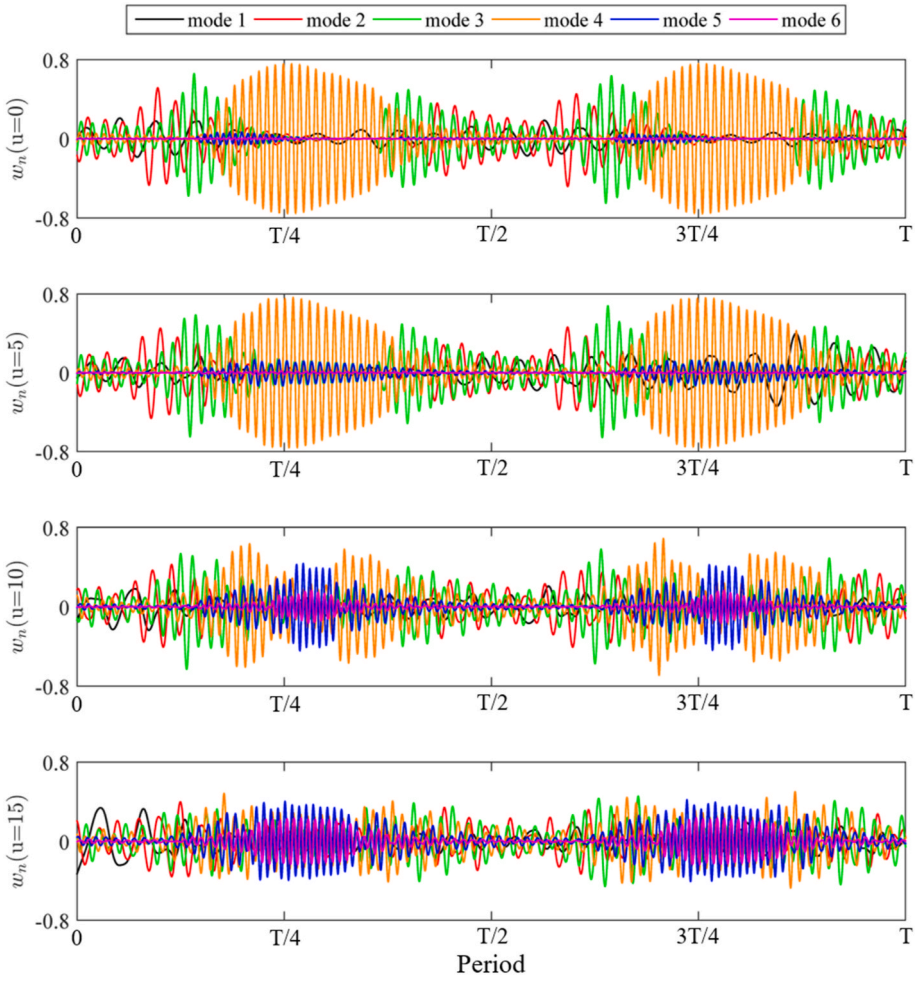

Fig. 14. The modal weights from mode 1 to mode 6 with the increase of non-dimensional internal flow velocity in one period of external oscillatory flow velocity.

CF VIV under external oscillatory flow. As demonstrated in Fig. 14, it can be observed that with the increase of the non-dimensional internal flow velocity u, high mode responses are triggered while the oscillatory flow velocity is approaching to its maximum. When $u = 0$ and 5, the 4th mode response of CF VIV is captured at around the maximal oscillatory flow velocity. As u is increased up to 10 and 15, the 5th mode response is detected for CF VIV while the external oscillatory flow velocity varies at around its maximum. It should be noticed that although the 6th mode response is not excited, its modal weight shows an increasing trend when u ranges from 10 to 15. The excitation of the new high mode response can be attributed to the decrease of the natural frequencies of the flexible fluid-conveying riser due to the increase of the non-dimensional internal flow velocity u. As high natural frequencies are reduced with the increase of u, the corresponding high mode responses are easily triggered while the external oscillatory flow velocity varies with time, resulting in the occurrence of high mode responses.

4.1.2. *The excited modes with different density ratios*

As for CF VIV dynamics of the flexible fluid-convey riser with different density ratio β of the internal and external flows, typical VIV features, such as hysteresis, mode transition and VIV developing process, can also be captured while the flexible fluid-conveying riser is subjected to the external oscillatory flow. The reason for these phenomena is due to the change of the oscillatory flow velocity too.

As the external oscillatory flow velocity is increased or decreased regardless of the density ratio β, mode transition occurs due to the excitation of various mode responses. When the density ratio β is low, relatively low mode response is mainly triggered with the external oscillatory flow velocity reaching its maximum. As shown in Fig. 15, CF VIV is dominated by the 4th mode response at around maximal oscillatory flow velocity for $\beta = 1$. When β is increased up to 2 and 3, the 5th mode response takes over CF VIV dynamics at around maximal oscillatory flow velocity. As the density ratio β continues to increase, higher mode response can be observed. It can be seen from Fig. 15 that the 6th mode response occurs when $\beta = 4$. It should be noticed that although the 7th mode response is not triggered, the modal weight of it is increased obviously when $\beta = 4$. Such change can be explained by that the increase of the density ratio β contributes to the decrease of the natural frequencies, leading to the appearance of high mode responses of the flexible fluid-conveying riser.

Similarly, the transition of excitation mode response of VIV with the increase of internal flow velocity (Meng et al. (2017); Yang et al. (2018); Jiang et al. (2019); Yuan et al. (2021)) and density (Thorsen et al. (2019); Li et al. (2020); Liang and Lou (2020); Duan et al. (2021a, 2021b)) is also observed by many investigators. In their researches, high mode response for VIV under uniform and shear currents is found triggered while the internal flow velocity and density is increased at the same external flow velocity, which can also be attributed to the decrease of natural frequencies. As the natural frequencies are reduced, the vortex shedding frequency is locked onto the newly decreased natural frequency of the flexible fluid-conveying riser, thereby leading to the excitation of new mode CF VIV response. Although the external oscillatory flow velocity is time-varying, high mode CF VIV response is obviously detected with high internal flow velocity and density under the same external oscillatory flow velocity. Moreover, due to the complexity of external oscillatory flow, CF VIV response of a flexible

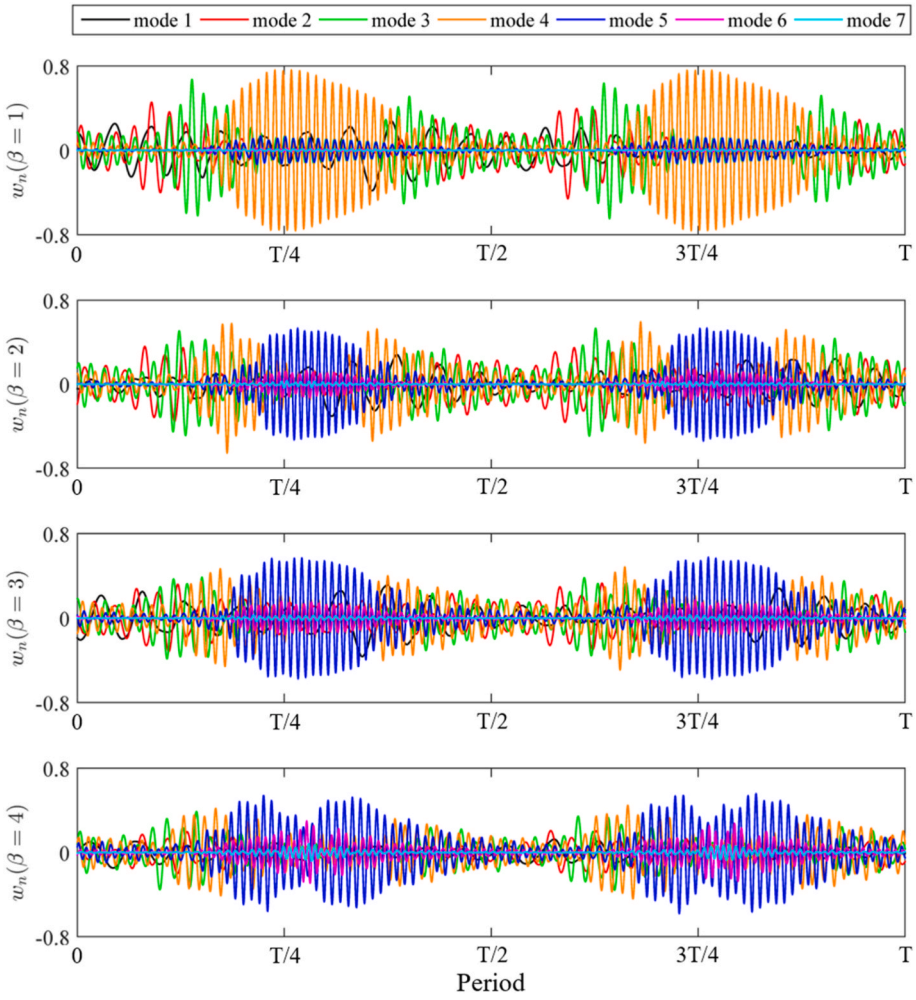

Fig. 15. The modal weights from mode 1 to mode 7 with the increase of density ratio in one period of external oscillatory flow velocity.

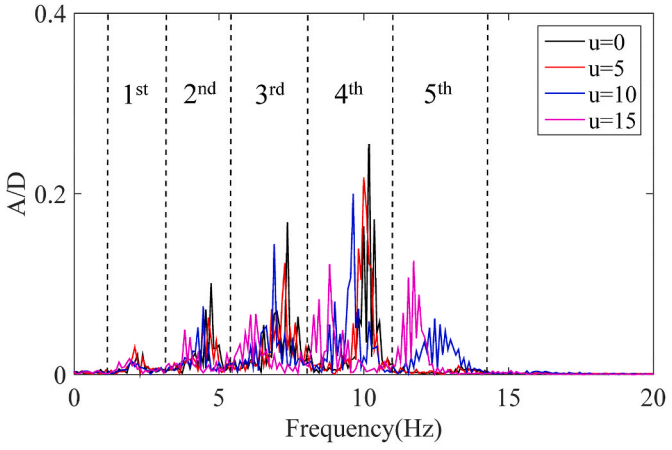

Fig. 16. The vibrating frequencies with the increase of non-dimensional internal flow velocity.

fluid-conveying riser is more complicated compared with that considering internal flow and uniform flow or shear flow.

4.2. The vibrating frequency for CF VIV considering internal flow and external oscillatory flow

The changing trend of the vibrating frequency of CF VIV with different non-dimensional internal flow velocities and density ratios is mainly analyzed and discussed in this subsection. CF VIV frequency and its distribution varying with time considering internal flow and external oscillatory flow are obtained based on the fast fourier transform and continuous wavelet transform techniques.

4.2.1. The vibrating frequency with different non-dimensional internal flow velocities

Firstly, CF VIV frequency of the fluid-conveying riser undergoing oscillatory flow is illustrated in Fig. 16 with the change of the non-dimensional internal flow velocity. Obviously, multi-frequency response is detected for the CF VIV with all non-dimensional internal flow velocity u. For the non-dimensional internal flow velocity $u = 0$ and

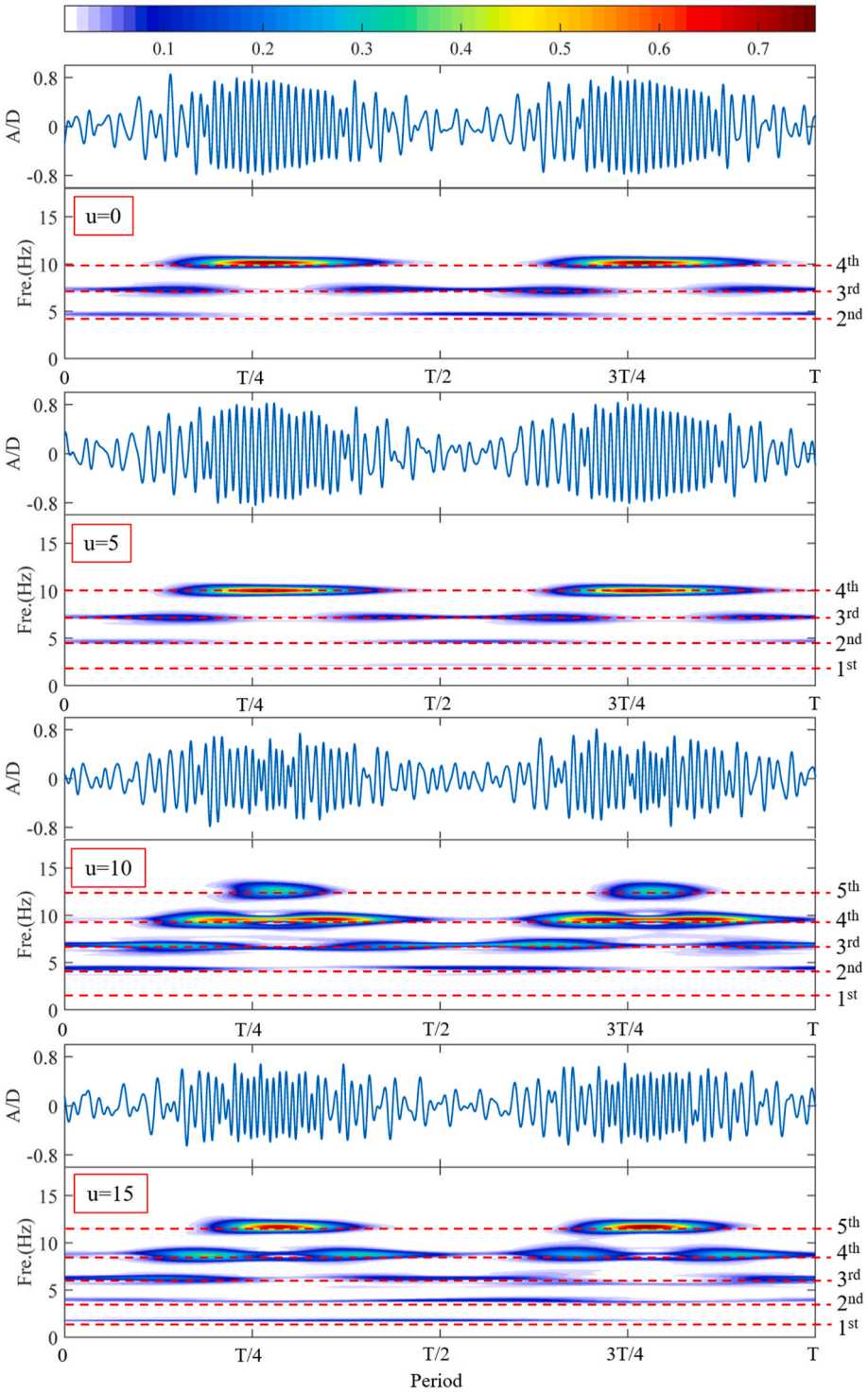

Fig. 17. VIV time history and vibrating frequency distribution with the increase of non-dimensional internal flow velocity in one period of external oscillatory flow.

5, the first four frequencies are observed, as shown in Fig. 16. With the increase of u, new vibrating frequency occurs. It can be seen from Fig. 16 that as u is increased up to 10 and 15, the 5th frequency corresponding to the 5th mode response appears accompanied with the first four vibrating frequencies with the change of external oscillatory flow velocity. It should be noted that the vibrating frequency of CF VIV shows a decreasing trend with the increase of u. This phenomenon is pretty evident while the non-dimensional internal flow velocity u is equal to 10 and 15. As is observed, the vibrating frequency decreases from approximately 4.45Hz, 6.91Hz, 9.64Hz and 12.45Hz to 3.82Hz, 6.09Hz, 8.82Hz and 11.73Hz when u increases from 10 to 15. The reason for this change is similar to the one leading to mode transition. As the non-dimensional internal flow velocity increases, the natural frequency of the flexible fluid-conveying riser is reduced. As a consequence, the vortex shedding frequency is locked onto the new decreased natural frequency, which causes the decrease of the vibrating frequency for CF VIV under external oscillatory flow. When the natural frequency corresponding to the certain high mode response is reduced to a certain value, the new high mode response is triggered, resulting in the appearance of the new vibrating frequency.

The time history and vibrating frequency distribution of CF VIV response with different non-dimensional internal flow velocity within one period of the external oscillatory flow are depicted in Fig. 17. It can be found from Fig. 17 that CF VIV dynamics of the flexible fluid-conveying riser subjected to external oscillatory flow is characterized by intermittent VIV, amplitude modulation as well as mode and frequency transitions.

Since the current velocity of the external oscillatory flow is time-varying, VIV response changes with time, leading to intermittent VIV. As indicated in Fig. 17, when the external oscillatory flow velocity is varying around 0, minimal VIV amplitude is observed regardless of the non-dimensional internal flow velocity. That manifests that the vibrating amplitude of CF VIV dynamics shows periodic features with the change of the external oscillatory flow velocity, thereby causing the intermittent VIV.

In addition, the vibrating amplitude of CF VIV is modulated as the external oscillatory flow velocity increases or decreases instantaneously. It can be observed from Fig. 17 that the vibrating amplitude of CF VIV is amplified with the increase of the external oscillatory flow velocity while the reduction of the external oscillatory flow velocity results in the decrease of VIV amplitude. This phenomenon can be explained by that as the current velocity of oscillatory flow is increased, the external hydrodynamic force exerting on the riser is enlarged, leading to the magnification of VIV amplitude. Similarly, the decrease of external hydrodynamic force due to the reduction of the external oscillatory flow velocity diminishes the vibrating amplitude.

It should be noticed that the vibrating frequency is not always continuous with variation of the external oscillatory flow velocity. Obviously, regardless of the non-dimensional internal flow velocity u, there exists frequency transition while the external oscillatory flow velocity varies with time, which can be seen in Fig. 17. When $u = 0$ and 5, the vibrating frequency jumps among response frequency corresponding to the 1st, 2nd, 3rd and 4th mode responses. The reason for this phenomenon lies in the excitation of new mode response with the variation of external oscillatory flow velocity. Besides, multi-frequency vibration is more notable at the moment when mode transition occurs for CF VIV response. As shown in Fig. 17, the 2nd, 3rd and 4th frequencies can be detected at the same moment while $u = 10$ and 15. This can be attributed to that though the certain high mode response is excited with the increase of the external oscillatory flow velocity, it requires time for the existing low mode response to decay. As a result, multi-frequency response can be detected due to the existence of more than one mode response when mode transition appears for CF VIV dynamics.

As for the effect of the internal flow, it is demonstrated in Fig. 17 that frequency transition still exists. And with the increase of the non-dimensional internal flow velocity u, high vibrating frequency can be captured for VIV response. For instance, when the non-dimensional internal flow velocity u is increased up to 10 and 15, the 5th vibrating frequency can be detected at approximately oscillatory flow velocity maximum. In addition, with the increase of u, the duration time for high mode response lasts longer. Such phenomenon can be observed more evidently for $u = 10$ and 15. This is because the increase of the non-dimensional internal flow velocity contributes to the decrease of the natural frequency of the flexible fluid-conveying riser, thereby leading to the new excitation of high mode response for CF VIV.

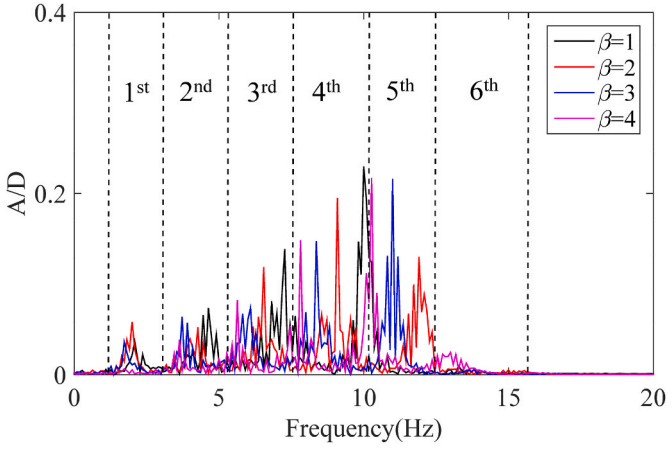

Fig. 18. The vibrating frequencies with the increase of density ratio.

4.2.2. *The vibrating frequency with different density ratios*

Likely, with the increase of the density ratio β between the internal and external flows, the variation of the vibrating frequency for CF VIV under external oscillatory flow is demonstrated in Fig. 18. It can be seen that multi-frequency VIV dynamics is detected with various density ratios β. When $\beta = 1$, the first four vibrating frequencies are detected. As the density ratio β is increased up to 2 and 3, the 5th frequency of 11Hz and 10.27Hz appears, respectively. With the value of β equal to 4, the 6th mode response is triggered, which is also accompanied by the first five mode responses. As a consequence, the 6th vibrating frequencies of 13Hz is detected for $\beta = 4$ while the external oscillatory flow velocity varies around its maximum, as shown in Fig. 18. Note that with the increase of the density ratio β, the existing frequencies decrease due to the change of the natural frequency of the flexible fluid-conveying riser. The decease of the vibrating frequency and occurrence of new vibrating frequency can be also attributed to the decrease of the natural frequency due to the increase of density ratio β.

The time history as well as the vibrating frequency distribution of CF VIV with the variation of the density ratio β between the internal and external flows is also presented in Fig. 18. Regardless of the density ratio, similar changing trend can be observed for VIV vibrating frequency and time history with the variation of the external oscillatory flow velocity, compared with that in last subsection. As indicated in Fig. 19, intermittent VIV and amplitude modulation are also captured due to the variation of the external oscillatory flow velocity. Besides, the vibrating frequency of CF VIV jumps among various frequencies, which can also be attributed to the excitation of different mode responses under different external oscillatory flow velocities. Meanwhile, with the increase of the density ratio β, new vibrating frequency is detected. As is demonstrated in Fig. 19, the 5th frequency corresponding to the 5th mode response appears at around the maximum of the external oscillatory flow velocity when the density ratio is increased up to 2 and 3. As the density ratio β keeps increasing, the 6th frequency is captured for $u = 4$ while the external oscillatory flow velocity is approaching to its maximum. The reason for this phenomenon is that the increase of the density ratio contributes to decrease the natural frequency, thereby resulting in the excitation of new mode response of CF VIV.

Likewise, the vibrating frequencies of VIV under uniform or shear currents show a decreasing trend while the internal flow velocity (Meng et al. (2017); Yang et al. (2018); Jiang et al. (2019); Yuan et al. (2021)) and density (Thorsen et al. (2019); Li et al. (2020); Liang and Lou (2020); Duan et al. (2021a, 2021b)) are increased. As is explained above, the natural frequencies of the flexible fluid-conveying riser are decreased with the increase of internal flow velocity and density. Since the vibrating frequencies for CF VIV are related to natural frequencies, their values are reduced too. The results prove that regardless of the type of external flow, the vibrating frequencies for VIV decrease with the increase of internal flow velocity and density.

4.3. *Standing and travelling wave responses considering internal flow and external oscillatory flow*

The standing and travelling wave responses of CF VIV considering both internal flow and external oscillatory flow are depicted in Figs. 20 and 21. It can be observed that both standing and travelling wave responses for CF VIV can be captured while the flexible fluid-conveying riser undergoes external oscillatory flow.

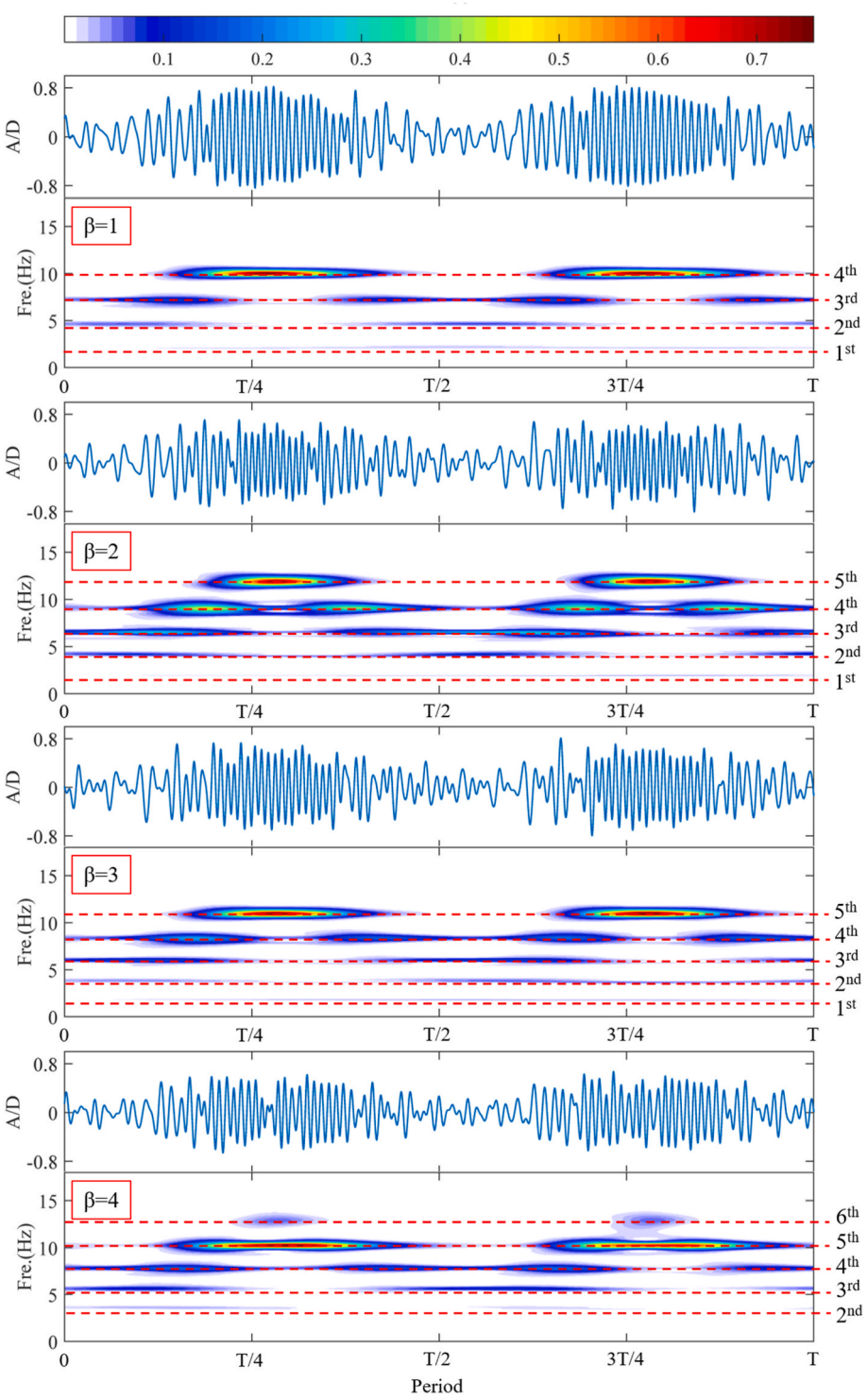

Fig. 19. VIV time history and vibrating frequency distribution with the increase of density ratio in one period of external oscillatory flow.

4.3.1. Standing and travelling wave responses with different non-dimensional internal flow velocities

Clearly, the travelling wave response can be notably detected when mode transition for CF VIV occurs. As shown in Fig. 20, the 1st,2nd and 3rd VIV responses are mainly dominated by the travelling wave response for $u = 0$. While the 4th mode response of CF VIV is triggered at around maximal oscillatory flow velocity, standing wave response dominates the CF VIV dynamics, accompanied with steady structural vibration. The reason for the dominance of travelling wave response for the low mode response of CF VIV can be explained by that the time duration is too short, leading to the unsteady VIV due to mode transition. While no mode transition occurs for the excited mode response, CF VIV is mainly dominated by standing wave response.

With the increase of the non-dimensional internal flow velocity u, travelling wave response can be detected more obviously. Besides, mode jump phenomenon can be evidently seen in Fig. 20. With $u = 0$ and 5, CF VIV response dominated by the 4th mode response appears as travelling wave response when the external oscillatory current velocity is approaching to its maximum. As the non-dimensional internal flow velocity is increased up to 10 and 15, the dominated mode response jumps

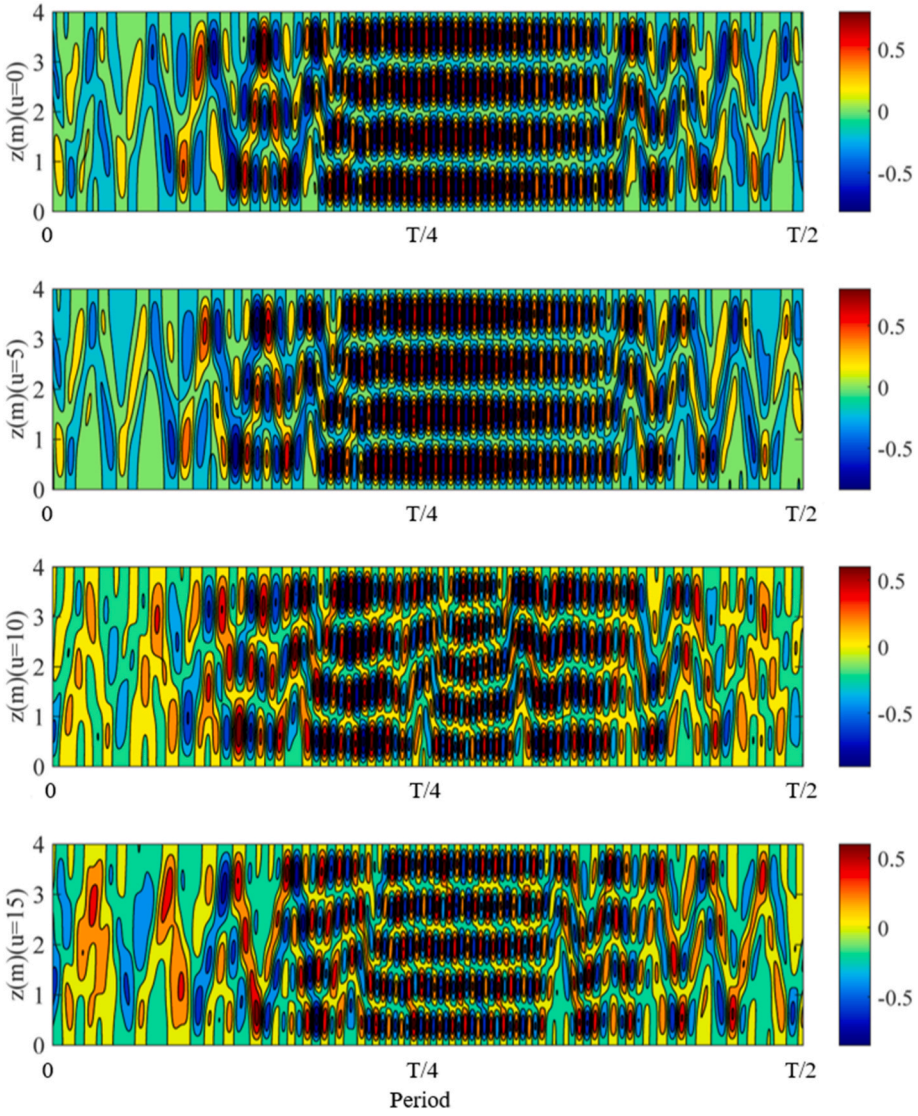

Fig. 20. Contour of the non-dimensional CF displacement in time and space with the increase of non-dimensional internal flow velocity in half period of external oscillatory flow.

to the 5th mode response at approximately oscillatory flow maximal velocity. And standing wave response dominates the 5th mode response when the flexible fluid-conveying riser vibrates steadily, as indicated in Fig. 20.

4.3.2. Standing and travelling wave responses with different density ratios

The standing and travelling wave responses of CF VIV dynamics are also affected by the density ratio β between the internal and external flows, as demonstrated in Fig. 21. With density ratio β equal to 1, VIV dynamics is dominated by the 4th mode response accompanied by the standing wave response while the external oscillatory flow velocity reaches its maximum. Nevertheless, travelling wave response is mainly captured for other low mode responses, especially at the moment when mode transition occurs. As the density ratio β increases to 2 and 3, standing wave response is mainly observed for the 5th mode response. It should be noted that travelling wave response appears accompanied with mode transition. However, VIV mainly presents characteristics of standing wave response while no mode transition occurs.

5. Conclusions

In this paper, CF VIV dynamics of a flexible riser considering both internal flow and external oscillatory flow is investigated based on the finite element method. The model applied here is firstly validated by comparison of the numerical results and experimental data, which proves the accuracy of the predicted results. Correspondingly, some nonlinear VIV characteristics, such as the excited mode, frequency, standing and travelling wave responses, are mainly focused and analyzed while the non-dimensional internal flow velocity and density ratio between the internal and external flows are changed. And some conclusions are drawn as follows:

Compared with VIV considering both internal flow and external uniform or shear current, VIV of a flexible fluid-conveying riser exposed to external oscillatory flow is more complicated. Regardless of the non-dimensional internal flow velocity and density ratio, some notable VIV features of the flexible fluid-conveying riser undergoing external oscillatory flow can be captured, such as hysteresis, intermittent VIV, amplitude modulation, mode and frequency transition. In addition, VIV developing process can be observed evidently, including building-up, lock-in and dying out. Standing and travelling wave responses can also be observed for CF VIV response. Moreover, travelling wave response mostly appears accompanied with mode transition. And the change of the external oscillatory current velocity mainly contributes to these VIV characteristics.

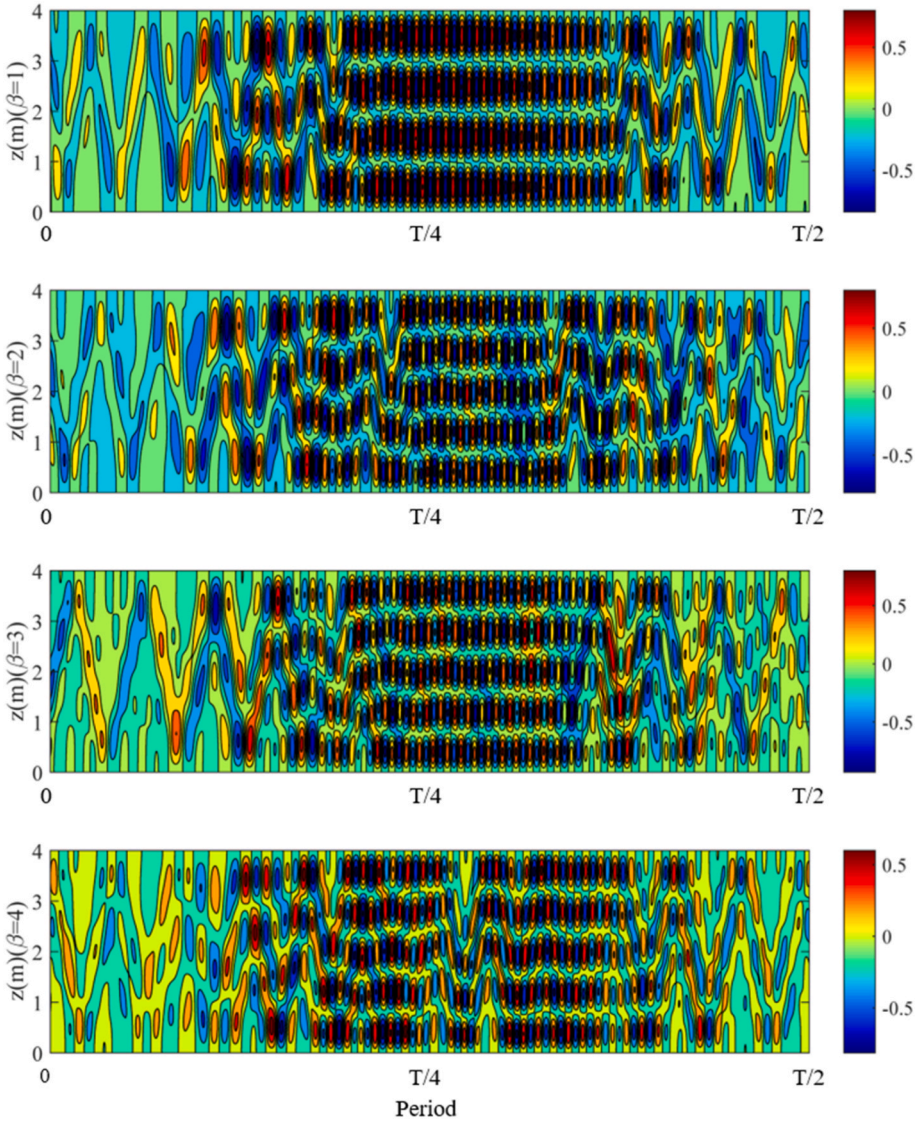

Fig. 21. Contour of the non-dimensional CF displacement in time and space with the increase of density ratio in half period of external oscillatory flow.

As the internal flow is taken into account, higher mode response can be effortlessly triggered with the increase of non-dimensional internal flow velocity and density ratio while the external oscillatory flow velocity is approaching to its maximum. Multi-frequency response can be detected for CF VIV under external oscillatory flow. Meanwhile, frequency transition occurs together with mode jump. As the non-dimensional internal flow velocity and density ratio are increased, the vibrating frequency decreases. Besides, standing and travelling wave response is also affected by the increase of non-dimensional internal flow velocity and density ratio.

This study mainly investigates CF VIV dynamics of a flexible fluid-conveying riser subjected to external oscillatory flow, which would help to enhance the understanding of VIV mechanism considering both internal flow and external oscillatory flow. It should be mentioned that KC number has a notable effect on vortex shedding, especially when the KC number is small. As the KC number in our investigation is larger than 30, the vortex shedding period is regarded small enough compared with the external flow oscillation period, which means that hydrodynamic force fluctuation due to the transient variation of the vortices shed from the riser can be ignored when external flow reverses (Blevins (1990); Sumer and Fredsoe (2006)). With such ignorance of hydrodynamic force change during external flow reversal, the hydrodynamic coefficients obtained from steady flow can be applied. It can be concluded that the numerical results with KC number higher than 30 are reliable in our work.

Nonetheless, the transient hydrodynamic force due to external flow reversal should be paid more attention too, particularly for the case of low KC number. Therefore, future works should be carried out to focus on hydrodynamic forces exerted on the riser undergoing oscillatory flow so that relationship between the transient hydrodynamic forces and other parameters (such as oscillatory flow velocity, amplitude and period as well as some structural parameters) can be explored with a variety of KC numbers quantitively and qualitatively. Then the establishment of hydrodynamic coefficient database under external oscillatory flow should be attempted, especially when the riser is subjected to external oscillatory flow with small KC numbers. Correspondingly, reliable hydrodynamic coefficients can be provided to calculate the hydrodynamic forces acting on a riser exposed to oscillatory flow for numerical investigation in future.

CRediT authorship contribution statement

Jinlong Duan: Conceptualization, Methodology, Investigation, Software, Validation, Data curation, Visualization, Writing – original

draft, Writing – review & editing. **Jifu Zhou:** Conceptualization, Methodology, Funding acquisition, Supervision, Visualization, Writing – review & editing. **Xu Wang:** Funding acquisition, Writing – review & editing. **Yunxiang You:** Conceptualization, Methodology. **Xinglan Bai:** Writing – review & editing.

Declaration of competing interest

The authors declare that they have no known competing financial interests or personal relationships that could have appeared to influence the work reported in this paper.

Acknowledgement

The authors acknowledge the supports of the National Natural Science Foundation of China (Grants 12132018 and 11972352) and the Strategic Priority Research Program of the Chinese Academy of Sciences (Grant XDA22040304).

References

Aronsen, K.H., 2007. An Experimental Investigation of In-Line and Combined In-Line and Cross-Flow Vortex Induced Vibrations[D], PhD Thesis. Department of Marine Technology, NTNU, Trondheim, Norway.
Bao, Y., Zhu, H.B., Huan, P., Wang, R., Zhou, D., Han, Z.L., Sherwin, S., 2019. Numerical prediction of vortex-induced vibration of flexible riser with thick strip method[J]. J. Fluid Struct. 89, 166–173.
Bao, J., Chen, Z.S., 2021. Vortex-induced vibration characteristics of multi-mode and spanwise waveform about flexible pipe subject to shear flow[J]. Int. J. Naval Architect. Ocean Eng. 13, 163–177.
Bearman, P.W., 2011. Circular cylinder wakes and vortex-induced vibrations[J]. J. Fluid Struct. 27 (5–6), 648–658.
Blevins, R.D., 1990. Flow-induced vibration[M]. Van Nostrand Reinhold, New York.
Blevins, R.D., Coughran, C.S., 2009. Experimental investigation of vortex-induced vibration in one and two dimensions with variable mass, damping, and Reynolds number [J]. J. Fluid Eng. 131, 101202, 1-7.
Bourguet, R., Karniadakis, G.E., Triantafyllou, M.S., 2011. Lock-in of the vortex-induced vibrations of a long tensioned beam in shear flow[J]. J. Fluid Struct. 27 (5–6), 838–847.
Chaplin, J.R., King, R., 2018. Laboratory measurements of the vortex-induced vibrations of an untensioned catenary riser with high curvature[J]. J. Fluid Struct. 79, 26–38.
Chen, W.L., Ji, C.N., Xu, D., Zhang, Z., Wei, Y., 2020. Flow-induced vibrations of an equilateral triangular prism at various angles of attack[J]. J. Fluid Struct. 97, 103099.
Dahl, M.J., 2008. Vortex-Induced Vibration of a Circular Cylinder with Combined In-Line and Cross-Flow Motion[D]. PhD Thesis. Department of Ocean Engineering, Massachusetts Institute of Technology, Cambridge, MA, USA.
Duan, J.L., Chen, K., You, Y.X., Li, J.L., 2018. Numerical investigation of vortex-induced vibration of a riser with internal flow[J]. Appl. Ocean Res. 72, 110–121.
Duan, J.L., Zhou, J.F., You, Y.X., Wang, X., 2021a. Time-domain analysis of vortex-induced vibration of a flexible mining riser transporting flow with various velocities and densities[J]. Ocean Eng. 220, 108427.
Duan, J., Zhou, J., You, Y., et al., 2021b. Effect of internal flow on vortex-induced vibration dynamics of a flexible mining riser in external shear current[J]. Mar. Struct. 80, 103094.
Evangelinos, C., Lucor, D., Karniadakis, G.E., 2000. DNS-derived force distribution on flexible cylinders subject to vortex-induced vibration[J]. J. Fluid Struct. 14 (3), 429–440.
Fu, S.X., Wang, J.G., Baarholm, R., Wu, J., Larsen, C.M., 2014. Features of vortex-induced vibration in oscillatory flow[J]. J. Offshore Mech. Arctic Eng. 136 (1), 011801.
Fu, B.W., Zou, L., Wan, D.C., 2018. Numerical study of vortex-induced vibrations of a flexible cylinder in an oscillatory flow[J]. J. Fluid Struct. 77, 170–181.
Gao, Y., Fu, S.X., Ren, T., Xiong, Y., Song, L.J., 2015. VIV response of a long flexible riser fitted with strakes in uniform and linearly sheared currents[J]. Appl. Ocean Res. 52, 102–114.
Gao, Y., Zou, L., Zong, Z., Takagi, S., Kang, Y., 2019. Numerical prediction of vortex-induced vibrations of a long flexible cylinder in uniform and linear shear flows using a wake oscillator model[J]. Ocean Eng. 171, 157–171.
Gopalkrishnan, R., 1993. Vortex-induced Forces on Oscillating Bluff Cylinders. Ph. D thesis, Massachusetts Institute of Technology, Cambridge, MA, USA.
Govardhan, R., Williamson, C., 2006. Defining the 'modified Griffin plot'in vortex-induced vibration: revealing the effect of Reynolds number using controlled damping [J]. J. Fluid Mech. 561, 147–180.
Guo, H.Y., Lou, M., 2008. Effect of internal flow on vortex-induced vibration of risers[J]. J. Fluid Struct. 24 (4), 496–504.
Huera-Huarte, F.J., Bangash, Z.A., Gonzalez, L.M., 2014. Towing tank experiments on the vortex-induced vibrations of low mass ratio long flexible cylinders[J]. J. Fluid Struct. 48, 81–92.
Jiang, T.Y., Liu, Z., Dai, H.L., Wang, L., He, F., 2019. Nonplanar multi-modal vibrations of fluid-conveying risers under shear cross flows[J]. Appl. Ocean Res. 88, 187–209.
Jauvtis, N., Williamson, C., 2004. The effect of two degrees of freedom on vortex-induced vibration at low mass and damping [J]. J. Fluid Mech. 509, 23–62.
Kheiri, M., Païdoussis, M.P., Del Pozo, G.C., Amabili, M., 2014. Dynamics of a pipe conveying fluid flexibly restrained at the ends[J]. J. Fluid Struct. 49, 360–385.
Li, Y.L., Guo, S.Q., Chen, W.M., 2018. Analysis on multi-frequency vortex-induced vibration and mode competition of flexible deep-ocean riser in sheared fluid fields [J]. J. Petrol. Sci. Eng. 163, 378–386.
Li, F.Q., An, C., Duan, M.L., Su, J., 2020. Combined damping model for dynamics and stability of a pipe conveying two-phase flow[J]. Ocean Eng. 195, 106683.
Li, X.M., Wei, W.F., Bai, F.T., 2020. A full three-dimensional vortex-induced vibration prediction model for top-tensioned risers based on vector form intrinsic finite element method[J]. Ocean Eng. 218, 108140.
Liang, W., Lou, M., 2020. Numerical simulation of vortex-induced vibration of a marine riser with a multiphase internal flow considering hydrate phase transition[J]. Ocean Eng. 216, 107758.
Lu, Z.Q., Fu, S.X., Zhang, M.M., Ren, H.J., 2019. An efficient time-domain prediction model for vortex-induced vibration of flexible risers under unsteady flows[J]. Mar. Struct. 64, 492–519.
Meng, S., Zhang, X., Che, C., Zhang, W., 2017. Cross-flow vortex-induced vibration of a flexible riser transporting an internal flow from subcritical to supercritical[J]. Ocean Eng. 139, 74–84.
Obasaju, E.D., Bearman, P.W., Graham, J.M.R., 1988. A study of forces, circulation and vortex patterns around a circular cylinder in oscillating flow[J]. J. Fluid Mech. 196, 467–494.
Païdoussis, M.P., 2014. Fluid-structure interactions, slender structures and axial flow [M], , Second ed.Volume 1. Academic Press, California, USA.
Passano, E., Larsen, C.M., Lie, H., Wu, J., 2016. VIVANA—Theory Manual Version 4.8. Trondheim, Norway.
Qu, Y., Metrikine, A.V., 2020. A wake oscillator model with nonlinear coupling for the vortex-induced vibration of a rigid cylinder constrained to vibrate in the cross-flow direction[J]. J. Sound Vib. 469, 115161.
Sarpkaya, T., 2004. A critical review of the intrinsic nature of vortex-induced vibrations [J]. J. Fluid Struct. 19 (4), 389–447.
Song, J.N., Lu, L., Teng, B., Park, H.I., Tang, G.Q., Wu, H., 2011. Laboratory tests of vortex-induced vibrations of a long flexible riser pipe subjected to uniform flow. Ocean Eng. 38 (11–12), 1308–1322.
Srinil, N., Zanganeh, H., Day, A., 2013. Two-degree-of-freedom VIV of circular cylinder with variable natural frequency ratio: experimental and numerical investigations[J]. Ocean Eng. 73, 179–194.
Sumer, B.M., Fredsoe, J., 1988. Transverse Vibrations of an Elastically Mounted Cylinder Exposed to an Oscillating flow[J].
Sumer, B.M., Fredsoe, J., 2006. Hydrodynamics Around Cylindrical Structures. World scientific.
Sun, X., Suh, C.S., Ye, Z.H., Yu, B., 2020. Dynamics of a circular cylinder with an attached splitter plate in laminar flow: a transition from vortex-induced vibration to galloping[J]. Phys. Fluids 32 (2), 027104.
Thorsen, M.J., Sævik, S., Larsen, C.M., 2014. A simplified method for time domain simulation of cross-flow vortex-induced vibrations[J]. J. Fluid Struct. 49, 135–148.
Thorsen, M.J., Sævik, S., Larsen, C.M., 2015. Fatigue damage from time domain simulation of combined in-line and cross-flow vortex-induced vibrations[J]. Mar. Struct. 41, 200–222.
Thorsen, M.J., Sævik, S., Larsen, C.M., 2016. Time domain simulation of vortex-induced vibrations in stationary and oscillating flows[J]. J. Fluid Struct. 61, 1–19.
Thorsen, M.J., Challabotla, N.R., Sævik, S., Nydal, O.J., 2019. A numerical study on vortex-induced vibrations and the effect of slurry density variations on fatigue of ocean mining risers[J]. Ocean Eng. 174, 1–13.
Trim, A.D., Braaten, H., Lie, H., Tognarelli, M.A., 2005. Experimental investigation of vortex-induced vibration of long marine risers[J]. J. Fluid Struct. 21 (3), 335–361.
Vandiver, J.K., Li, L., 2018. User Guide for SHEAR7 Version 4.10a. Massachusetts Institute of Technology, Cambridge, MA, USA.
Violette, R., Langre, E., de Szydlowski, J., 2010. A linear stability approach to vortex-induced vibrations and waves[J]. J. Fluid Struct. 26 (3), 442–466.
Wang, E.H., Xiao, Q., 2016. Numerical simulation of vortex-induced vibration of a vertical riser in uniform and linearly sheared currents[J]. Ocean Eng. 121, 492–515.
Wang, J.G., Fu, S.X., Baarholm, R., 2018. Evaluation of vortex-induced vibration of a steel catenary riser in steady current and vessel motion-induced oscillatory current [J]. J. Fluid Struct. 82, 412–431.
Wang, L., Dai, H.L., Qian, Q., 2012. Dynamics of simply supported fluid-conveying pipes with geometric imperfections[J]. J. Fluid Struct. 29, 97–106.
Wang, L., Jiang, T.L., Dai, H.L., Ni, Q., 2018. Three-dimensional vortex-induced vibrations of supported pipes conveying fluid based on wake oscillator models[J]. J. Sound Vib. 422, 590–612.
Williamson, C.H.K., 1985. In-line response of a cylinder in oscillatory flow[J]. Appl. Ocean Res. 7 (2), 97–106.
Williamson, C.H.K., Govardhan, R., 2008. A brief review of recent results in vortex-induced vibrations[J]. J. Wind Eng. Ind. Aerod. 96 (6–7), 713–735.
Xu, W.H., Ma, Y.X., Ji, C.N., Sun, C., 2018. Laboratory measurements of vortex-induced vibrations of a yawed flexible cylinder at different yaw angles[J]. Ocean Eng. 154, 27–42.
Xue, H.X., Yuan, Y.C., Tang, W.Y., 2019. Numerical investigation on vortex-induced vibration response characteristics for flexible risers under sheared-oscillatory flows [J]. Int. J. Naval Architect. Ocean Eng. 11 (2), 923–938.

Yang, W., Ai, Z., Zhang, X., Chang, X., Gou, R., 2018. Nonlinear dynamics of three-dimensional vortex-induced vibration prediction model for a flexible fluid-conveying pipe[J]. Int. J. Mech. Sci. 138, 99–109.
Yin, D., Passano, E., Lie, H., et al., 2019. Experimental and numerical study of a top tensioned riser subjected to vessel motion[J]. Ocean Eng. 171, 565–574.
Yuan, Y.C., Xue, H.X., Tang, W.Y., 2018. Numerical analysis of Vortex-Induced Vibration for flexible risers under steady and oscillatory flows[J]. Ocean Eng. 148, 548–562.
Yuan, Y., Xue, H., Tang, W., 2020a. A numerical investigation of vortex-induced vibration response and fatigue damage for flexible cylinders under combined uniform and oscillatory flow[J]. China Ocean Eng. 34 (4), 488–499.
Yuan, Y., Xue, H., Tang, W., 2020b. Nonlinear dynamic response analysis of marine risers under non-uniform combined unsteady flows[J]. Ocean Eng. 213, 107687.
Yuan, Y., Xue, H., Tang, W., 2021. Internal laminar flow effect on the nonlinear dynamic response of marine risers under uniform ocean current. Ships Offshore Struct. 1–10.
Zhang, M.M., Fu, S.X., Liu, C., Ren, H.J., Xu, Y.W., 2021. Experimental investigation on vortex-induced force of a Steel Catenary Riser under in-plane vessel motion[J]. Mar. Struct. 78 (8), 102882.
Zhao, M., 2013. Numerical investigation of two-degree-of-freedom vortex-induced vibration of a circular cylinder in oscillatory flow[J]. J. Fluid Struct. 39, 41–59.
Zheng, H.N., 2014. The Influence of High Harmonic Force on Fatigue Life and its Prediction via Coupled Inline-Crossflow VIV modeling[D]. Massachusetts Institute of Technology.
Zhu, H.J., Lin, P.Z., Gao, Y., 2019a. Vortex-induced vibration and mode transition of a curved flexible free-hanging cylinder in exponential shear flows[J]. J. Fluid Struct. 84, 56–76.
Zhu, H.J., Gao, Y., Zhao, H.L., 2018. Experimental investigation on the flow-induced vibration of a free-hanging flexible riser by internal unstable hydrodynamic slug flow[J]. Ocean Eng. 164, 488–507.
Zhu, H.J., Gao, Y., Zhao, H.L., 2019b. Coupling vibration response of a curved flexible riser under the combination of internal slug flow and external shear current[J]. J. Fluid Struct. 91, 102724.